

# Neuroprotective mechanisms of cobalamin in ischemic stroke insights from network pharmacology and molecular simulations

Received: 19 May 2025

Accepted: 20 February 2026

Published online: 02 March 2026

Cite this article as: Zhou L., Cai Y., Wu H. *et al.* Neuroprotective mechanisms of cobalamin in ischemic stroke insights from network pharmacology and molecular simulations. *Sci Rep* (2026). <https://doi.org/10.1038/s41598-026-41564-6>

Li Zhou, Yanli Cai, Haiyun Wu, Jiani Wang, Fangmei Xiao, Pingping Liu & Qin Yang

We are providing an unedited version of this manuscript to give early access to its findings. Before final publication, the manuscript will undergo further editing. Please note there may be errors present which affect the content, and all legal disclaimers apply.

If this paper is publishing under a Transparent Peer Review model then Peer Review reports will publish with the final article.

# Neuroprotective Mechanisms of Cobalamin in Ischemic Stroke Insights from Network Pharmacology and Molecular Simulations

Li Zhou<sup>1, #</sup>, Yanli Cai<sup>2, #</sup>, Haiyun Wu<sup>1</sup>, Jiani Wang<sup>1</sup>, Fangmei Xiao<sup>1</sup>, Pingping Liu<sup>1</sup>, Qin Yang<sup>1\*</sup>

<sup>1</sup> Department of Neurology, the First Affiliated Hospital of Chongqing Medical University, Chongqing, China

<sup>2</sup> Outpatient Department, Ziyang Central Hospital, Sichuan, China

**#Co-first author:** These authors contributed equally to this work and are co-first authors.

**\*Correspondence:** Professor Qin Yang, Department of Neurology, the First Affiliated Hospital of Chongqing Medical University, Chongqing 400016, China.

Email: xyqh200@126.com; Fax: 86-23-68811487; Telephone: 86-23-89012008.

Address: 1 Youyi Road, Yuzhong District, 400016, Chongqing, China

**Word count:** 5182 words.

**Number of references:** 72.

**Number of tables:** 3.

**Number of figures:** 9.

**Abstract**

**Purpose:** This study aims to systematically investigate the multi-target mechanisms of cobalamin in the treatment of ischemic stroke using network pharmacology and molecular docking approaches.

**Methods:** We screened databases to identify the targets of cobalamin and performed intersected with with ischemic stroke-related targets to construct a "drug-target-disease" interaction network. Gene Ontology (GO) and Kyoto Encyclopedia of Genes and Genomes (KEGG) pathway enrichment analyses were conducted to identify key biological processes and signaling pathways. Additionally, molecular docking simulations were performed to assess the binding affinity between cobalamin and hub proteins. Molecular dynamics (MD) simulations were used to assess the stability of the protein-ligand complexes over a 500 ns simulation period. Additionally, ADME (Absorption, Distribution, Metabolism, Excretion) and blood-brain barrier (BBB) permeability predictions were made using ADMETlab 3.0 and admetSAR 3.0.

**Results:** A total of 95 therapeutic targets of cobalamin for ischemic stroke were identified. Network analysis and molecular docking highlighted eight core targets—ALB, TIMP1, PLG, FN1, AGT, SERPINE1, APOE, and SPP1—with high binding affinities to cobalamin. GO analysis suggested that cobalamin regulates inflammatory responses, post-translational modifications, complement binding, and lipoprotein particle binding. KEGG analysis identified complement and coagulation cascades, the PI3K/AKT pathway, and inflammation-related signaling as central to its therapeutic effects. Molecular docking showed strong binding to ALB and TIMP1, which was further confirmed by MD simulations, with minimal conformational changes. The PLG-cobalamin complex exhibited more fluctuations. ADME analysis revealed low

passive permeability, particularly across the blood-brain barrier, but moderate distribution and high plasma protein binding.

**Conclusion:** This study provides evidence that cobalamin may offer neuroprotective effects in ischemic stroke by interacting with key target proteins involved in coagulation, inflammation, and lipid metabolism. The findings highlight the potential of cobalamin as a therapeutic agent, although its limited ability to cross the blood-brain barrier may restrict its oral use. Further experimental validation and development of suitable delivery methods are needed to fully realize cobalamin's potential in stroke therapy.

**Keywords:** Ischemic stroke, Cobalamin, Network pharmacology, Molecular Docking

## 1. Introduction

Ischemic stroke accounts for approximately 70% of all stroke cases and is responsible for more than 10 million deaths worldwide each year (<https://www.who.int/data/gho>). Its pathophysiology is highly complex, involving multiple interrelated processes such as oxidative stress, inflammation, neuronal apoptosis, and disruption of the blood-brain barrier (1, 2). Although reperfusion therapies, including recombinant tissue plasminogen activator (rt-PA) and endovascular thrombectomy, have demonstrated clinical efficacy when administered within a narrow therapeutic window, many patients still experience irreversible neurological deficits due to delayed treatment and the risk of reperfusion injury (3). Consequently, exploring neuroprotective agents with multi-target and multi-pathway regulatory effects has become a prominent area of research.

Cobalamin (vitamin B12) is a water-soluble vitamin essential for one-carbon metabolism and myelin synthesis. Emerging studies suggest that cobalamin may exert neuroprotective effects, including antioxidant, anti-inflammatory, anti-apoptotic, and mitochondrial regulatory functions (4, 5). Owing to these pleiotropic biological activities, cobalamin is hypothesized to modulate

multiple pathological processes involved in ischemic stroke (6). However, direct experimental evidence supporting this hypothesis remains limited. Notably, cobalamin deficiency has been associated with various neurological disorders, such as cognitive impairment, autism spectrum disorder, epilepsy, schizophrenia, depression, and migraine. Several studies have demonstrated that cobalamin supplementation can alleviate symptoms of these conditions (7-9). In addition, low serum cobalamin levels have been identified as an independent risk factor for ischemic stroke, and early supplementation has shown potential to improve neurological outcomes in stroke patients (10-12).

Traditional experimental approaches are often insufficient to fully elucidate the complex regulatory networks underlying ischemic stroke. In contrast, network pharmacology, which integrates target prediction, pathway analysis, and molecular docking, offers a systematic approach to explore the interactions between drugs, targets, and diseases, thereby providing novel insights into the therapeutic potential of cobalamin (13).

This study aims to: (1) identify the core targets of cobalamin in ischemic stroke through network pharmacology; (2) evaluate the binding affinity between cobalamin and key targets through molecular docking analysis; and (3) propose a multi-target regulatory framework to support future experimental validation. The findings are expected to establish a theoretical foundation for nutritional interventions and drug development strategies targeting ischemic stroke. An overview of the study workflow is presented in Figure 1.

## **2. Methods and materials**

### **2.1 Identification of targets of cobalamin**

Potential cobalamin targets were systematically retrieved from three databases in November 2024: DrugBank, GeneCards, and SwissTargetPrediction. For GeneCards, we retained only targets with relevance scores  $\geq 10$ , which was chosen based on previous studies that suggest a relevance score of 10 or higher is indicative of robust biological

evidence for the target's involvement in relevant pathways or diseases (14). For SwissTargetPrediction, a probability cutoff of  $\geq 0.5$  was used, in line with typical usage in predictive modeling, where a probability of  $\geq 0.5$  is considered a reasonable threshold for reliable predictions of drug-target interactions (15). All gene names were converted to official HUGO Gene Nomenclature Committee symbols via UniProt, and duplicates were removed after cross-database integration.

## **2.2 Identification of ischemic stroke disease targets**

Disease-related targets for ischemic stroke were identified by searching the GeneCards, DisGeNET, and OMIM databases. In the GeneCards database, targets with a relevance score  $\geq 10$  were selected to ensure high-confidence associations with ischemic stroke (14). In contrast, all associated genes from DisGeNET were included to provide broad coverage of potential mechanisms, as our aim was to capture a wide array of relevant genes without restricting the dataset based on score thresholds. This approach was chosen to avoid missing any potentially important genes linked to ischemic stroke. Similarly, relevant manually curated genes were retrieved from OMIM using the keyword "ischemic stroke."

Data from the three databases were integrated using a Venn diagram, and duplicate entries were removed to generate a comprehensive list of ischemic stroke-related targets. The potential therapeutic targets of cobalamin against ischemic stroke were then identified by cross-referencing these common ischemic stroke targets with known cobalamin targets using the Draw Venn Diagram online tool. Functional classification of the resulting therapeutic targets was conducted using the PANTHER classification system (accessed November 2024) (16).

## **2.3 PPI network construction and analysis**

The common cobalamin targets for ischemic stroke were analyzed using the DAVID database (accessed December 2024) for Gene Ontology (GO) and Kyoto Encyclopedia of Genes and Genomes (KEGG) enrichment analysis with

Benjamini-Hochberg FDR correction (17-19). Terms with  $P < 0.05$  and  $FDR < 0.05$ , containing at least 5 targets, were considered significant. Protein-protein interaction (PPI) networks were constructed using the STRING database (Homo sapiens; minimum interaction score: 0.7) and visualized in Cytoscape using a force-directed layout. Hub genes were identified as the top 10% based on degree centrality. The integrated functional network was then constructed and visualized (20).

#### **2.4 Molecular docking validation**

First, the crystal structure of the target protein was obtained from the PDB. PyMOL was used to remove water molecules, inorganic ions, and other non-essential components, and the processed structure was saved as the receptor file (21). The ligand molecule was retrieved from the PubChem database, converted to PDB format using PyMOL, and subsequently prepared by adding hydrogen atoms and charges. For target proteins with co-crystallized ligands, the active site was defined using the coordinates of the bound ligand. For proteins without co-crystallized ligands, potential binding pockets were predicted using the CASTp 3.0 server (<http://sts.bioe.uic.edu/castp/>), and the center of the largest predicted pocket was selected to define the docking grid. All docking grid boxes were then constructed using AutoDockTools, where the grid center coordinates and box dimensions were specified accordingly. Molecular docking was subsequently performed using AutoDock Vina (22). After docking, the binding conformation with the lowest binding energy was selected and analyzed. The receptor-ligand interactions were visualized using PyMOL (23). The URLs employed in this section are summarized in Table 1.

#### **2.5 Molecular dynamics simulations validation**

Based on the docking results, the optimal protein-ligand complex was subjected to molecular dynamics (MD) simulations using the GROMACS 5.0 package (24) with the CHARMM36 force field (24) under periodic boundary conditions. Ligand topology parameters were generated using the CHARMM General Force Field (CGenFF) (25). The system was solvated, neutralized by

the addition of counterions, and energy-minimized using the steepest descent algorithm to eliminate unfavorable contacts.

Electrostatic interactions were calculated using the particle mesh Ewald (PME) method, while van der Waals interactions were treated with a suitable cutoff scheme. The system was equilibrated sequentially in the NVT ensemble for 50,000 steps and then in the NPT ensemble for an additional 50,000 steps. Production MD simulations were subsequently conducted for 100 ns at 300 K with a time step of 2.0 fs, and trajectory coordinates were saved every 1 ps for further analysis (26, 27).

## **2.6 In silico prediction of ADME and blood-brain barrier properties of cobalamin**

Pharmacokinetic and other ADMET-related properties of cobalamin were predicted using two web-based tools, ADMETlab 3.0 (<https://admetlab3.scbdd.com/server/screening>) and admetSAR 3.0 (<https://lmmd.ecust.edu.cn/admetSar3/resource.php>). The canonical SMILES representation of cobalamin was obtained from PubChem, and gastrointestinal absorption, blood-brain barrier (BBB) permeability, volume of distribution, and other ADMET-related parameters were predicted under the default settings of each server.

## **3. Results**

### **3.1 Target identification for GO and KEGG enrichment analysis of cobalamin intervention in ischemic stroke**

A total of 2,216 cobalamin-related targets were initially retrieved from the GeneCards, DrugBank, and SwissTargetPrediction databases. Simultaneously, 2,262 ischemic stroke-associated targets were identified by searching the GeneCards and OMIM databases. By intersecting the cobalamin-related targets with those associated with ischemic stroke, 828 common targets were obtained (Figure 2A). Subsequently, a Venn diagram analysis between these 828 shared targets and our previously identified proteomic targets yielded 95

overlapping genes (Figure 2B). The functional categories of these 95 targets are shown in Figure 2C, including metabolite interconversion enzymes, protein-modifying enzymes, intercellular signaling molecules, transmembrane signal receptors, gene-specific transcriptional regulators, transporters, protein-binding activity modulators, cell adhesion molecules, defense/immunity proteins, and DNA metabolism proteins.

### 3.2 PPI network construction

To investigate the interactions among the therapeutic targets of cobalamin in ischemic stroke, a PPI network was constructed using the STRING database. (Figure 3A). The resulting interaction data were imported into Cytoscape v3.10.1 for visualization (Figure 3B). To further identify the core targets of cobalamin in the regulation of ischemic stroke, degree centrality (DC) was calculated using the CytoNCA plugin in Cytoscape. ALB, FN1, and CRP exhibited the highest DC values (Table 2) and were therefore selected as potential hub targets.

Subsequent GO enrichment analysis of these hub genes revealed that they are significantly involved in several biological processes, including fibrinolysis, negative regulation of coagulation, low-density lipoprotein particle remodeling, and acute-phase responses (Figure 3E, 3F, 3H). These functions align with the known pathological mechanisms of ischemic stroke and suggest that the identified hub genes may serve as critical targets through which cobalamin exerts its therapeutic effects. To explore the modular structure of the network, cluster analysis was performed using the MCODE plugin. Three distinct clusters were identified: Cluster 1 included 40 nodes and 437 edges (score = 22.410), Cluster 2 contained 27 nodes and 149 edges (score = 11.462), and Cluster 3 comprised 4 nodes and 6 edges (score = 4.000) (Figures 3C, 3D, 3G). GO biological process enrichment analysis was conducted for each cluster to characterize their functional significance. As illustrated in Figure 3E, proteins in Cluster 1 were primarily involved in the negative regulation of blood coagulation, acute-phase response, and blood coagulation. Proteins in Cluster

2 (Figure 3F) were mainly associated with blood coagulation, inflammatory response, negative regulation of fibrinolysis, and complement activation via the alternative pathway. Cluster 3 proteins (Figure 3H) were predominantly related to lipid transport, lipoprotein metabolic process, and triglyceride catabolic process.

Collectively, these results suggest that the core functional modules within the PPI network are mainly involved in coagulation cascades, inflammatory responses, and lipid metabolism. These biological processes are known to play critical roles in the pathogenesis and progression of ischemic stroke.

To further identify the key regulatory genes within the network, topological analysis was performed using the CytoHubba plugin in Cytoscape. Nodes were ranked using the Maximal Clique Centrality (MCC) algorithm, which is considered a robust method for hub gene identification. This analysis identified 10 hub genes: AGT, CRP, PLG, VWF, ALB, FN1, TIMP1, APOE, SPP1, and SERPINE1 (Figure 4A).

Subsequently, GO enrichment analysis was conducted for these hub genes. In the biological process (BP) category, the top five enriched terms were: symbiont-related biological processes, fibrinolysis, low-density lipoprotein particle remodeling, negative regulation of blood coagulation, and negative regulation of fibrinolytic processes (Figure 4B). In the cellular component (CC) category, the most significantly enriched terms included: platelet alpha granule lumen, extracellular space, extracellular region, extracellular exosome, and collagen-containing extracellular matrix (Figure 4C). For molecular function (MF) (Figure 4D), the top enriched terms were: protease binding, protein folding chaperone binding, receptor-ligand activity, signaling receptor binding, and integrin binding.

Notably, network centrality analysis using CytoNCA showed a high degree of consistency with the results obtained from CytoHubba, further validating the critical role of these hub genes. These genes are primarily involved in the regulation of key biological processes such as the coagulation cascade,

inflammatory response, and lipid metabolism, suggesting that they may play essential roles in the pathogenesis and progression of ischemic brain injury.

### **3.3 GO enrichment analysis**

Figure 5A illustrates the core hub genes potentially modulated by cobalamin in the context of ischemic stroke. GO enrichment analysis further revealed the involvement of these genes in key BP, CC, and MF. In the BP category, the top five enriched terms were: acute-phase response, interaction with symbiont, acute inflammatory response, platelet degranulation, and maintenance of location (Figure 5B). For the CC category, the most significantly enriched components included: platelet alpha granule lumen, platelet alpha granule, blood microparticle, endoplasmic reticulum lumen, and secretory granule lumen. In the MF category, the top five enriched functions were: chaperone binding, macrolide binding, toxic substance binding, opsonin binding, and low-density lipoprotein particle binding. In addition, the c-net network diagram (Figure 5C) provides a visual overview of the functional associations among these hub genes. These findings suggest that cobalamin may exert protective effects in ischemic stroke by modulating key biological processes such as the inflammatory response, post-translational protein modification, complement activation, and lipoprotein particle binding.

### **3.4 KEGG enrichment analysis**

KEGG pathway analysis provides key insights into the regulatory mechanisms underlying biological processes, thereby facilitating a more comprehensive understanding of the protective effects of cobalamin in ischemic stroke. As shown in Figure 6A, cobalamin appears to exert its effects primarily through several critical signaling pathways, including the complement and coagulation cascades, cholesterol metabolism, and ECM-receptor interaction pathways. Further KEGG enrichment analysis categorized these pathways into the following major functional groups (Figures 6B and 6C): Human disease-related pathways, such as the AGE-RAGE signaling pathway in diabetic complications, *Staphylococcus aureus* infection, proteoglycans in

cancer, various infectious diseases, and endocrine and metabolic disorders; Organismal systems, encompassing pathways involved in the immune system, digestive system, aging, complement and coagulation cascades, and cholesterol metabolism; Cellular processes, including phagosome formation, focal adhesion, ferroptosis, the p53 signaling pathway, cell growth and death, transport and catabolism, and cell-cell communication in eukaryotes; Environmental information processing, including ECM-receptor interaction, cytokine-cytokine receptor interaction, PI3K-Akt signaling pathway, signaling molecules and interaction, and signal transduction. Figure 6D illustrates a bubble plot of the top 20 significantly enriched pathways and their associated target genes, while Figure 6E displays a pathway-target network, with green nodes representing signaling pathways and yellow nodes indicating target genes. Taken together, these findings suggest that cobalamin may exert neuroprotective effects against ischemic stroke by modulating multiple pathways, particularly those involved in the complement and coagulation cascades, PI3K/Akt signaling, and other inflammation-related mechanisms. This highlights the potential of cobalamin as a multitarget therapeutic agent in the prevention and treatment of ischemic stroke.

### **3.5 Validation of interactions between cobalamin and potential targets through molecular docking**

To evaluate the binding affinity of cobalamin with the proteins encoded by the 10 hub genes, molecular docking analysis was performed. The docking model with the lowest binding energy ( $\Delta G$ ) was recorded for each ligand-target protein pair. Due to the lack of available docking sites for CRP and vWF in the AutoDock database, these two targets were excluded from the docking analysis. The docking results for the remaining eight target proteins are summarized in Table 3 and illustrated in Figure S1. Among them, cobalamin exhibited the strongest binding affinity with ALB and TIMP1, with ALB showing the most stable binding conformation. This was followed by PLG, FN1, AGT, SERPINE1, APOE, and SPP1. The specific binding sites between

cobalamin and each target protein are depicted in Figure S1. These results suggest that cobalamin may exert its protective effects in ischemic stroke, at least in part, by stably interacting with key hub proteins involved in the pathophysiology of the disease. It is noteworthy that ALB, TIMP1, PLG, and cobalamin exhibit the strongest binding energies in their interactions.

### **3.6 Molecular dynamics simulations of the core targets**

We employed MD simulations to evaluate the dynamic stability of receptor-ligand complexes under physiological conditions. Cobalamin was selected for simulation with ALB, TIMP1, and PLG to assess binding stability, considering factors such as binding affinity, complex interactions, and compound structural diversity. The stability of each system was evaluated by calculating the root mean square deviation (RMSD), root mean square fluctuation (RMSF), radius of gyration (Rg), and solvent accessible surface area (SASA) during a 500 ns simulation period. Additionally, Gibbs free energy landscape analysis was performed to further validate the binding stability of cobalamin with the target genes and to explore its potential neuroprotective mechanisms.

Through MD simulations, the ALB-Cobalamin and TIMPI-Cobalamin complexes exhibited high structural stability. The RMSD of ALB-Cobalamin was 1.0 nm (Figure 7A), while the RMSD of TIMPI-Cobalamin was even lower, around 0.5 nm, indicating minimal conformational changes. Ligand RMSD analysis showed that Cobalamin remained stable in both ALB-Cobalamin and TIMPI-Cobalamin complexes, with low RMSD values of 1.0 nm and 0.5 nm, respectively (Figure 7B). In contrast, the PLG-Cobalamin complex displayed a higher RMSD of 1.5 nm (Figure 7A), with the ligand RMSD fluctuating significantly, showing greater variation in Cobalamin's structure.

In the radius of gyration (Rg) analysis, the ALB-Cobalamin complex exhibited an Rg value of 3.0 nm (Figure 7C), suggesting a more extended conformation. In contrast, both PLG-Cobalamin and TIMPI-Cobalamin had smaller Rg values of 2.5 nm, indicating that these complexes are more compact and structurally stable (Figure 7C).

In the SASA analysis, the SASA values for all three complexes remained stable without significant changes, indicating that their surface properties did not undergo significant alterations during the simulations (Figure 7D).

In the RMSF analysis, ALB-Cobalamin showed considerable fluctuation, especially in the 100-300 residue region (Figure 8A), while TIMPI-Cobalamin exhibited small fluctuations, demonstrating overall high stability (Figure 8E). The RMSF of PLG-Cobalamin showed greater fluctuations (Figure 8C), indicating higher structural flexibility and larger variations in the region interacting with Cobalamin. The number of hydrogen bonds in ALB-Cobalamin remained around 1 (Figure 8B), while in PLG-Cobalamin, it fluctuated between 1 and 5 (Figure 8D), suggesting a more dynamic interaction with Cobalamin. The number of hydrogen bonds in TIMPI-Cobalamin remained relatively stable, between 2 and 3 (Figure 8F).

Finally, the Gibbs free energy landscape analysis revealed that the ALB-Cobalamin complex had its lowest energy point at PC1  $\sim$  0.4, PC2  $\sim$  2.8, suggesting a more extended conformation (Figure 9A, B, C). The free energy landscape of PLG-Cobalamin was more complex, showing multiple low-energy points, with the lowest energy region at PC1  $\sim$  0.8, PC2  $\sim$  3.0 (Figure 9D, E, F), suggesting the existence of multiple stable conformations. The TIMPI-Cobalamin free energy landscape displayed a deep and concentrated low-energy region, with the most stable conformation occurring at PC1  $\sim$  0.3, PC2  $\sim$  2.0 (Figure 9G, H, I), indicating a stable and less variable structure.

### **3.7 In silico ADME and blood brain barrier profile of cobalamin**

To characterize the pharmacokinetic profile of cobalamin at the computational level, we predicted its ADMET properties using ADMETlab 3.0 and admetSAR 3.0 (Table S1). Both platforms indicated that cobalamin has a very large molecular weight (approximately 1.3 kDa) and an extremely high topological polar surface area (TPSA  $\sim$  460-480  $\text{\AA}^2$ ), with good aqueous solubility, but clearly falls outside the typical physicochemical space of drug-like small molecules. With respect to absorption, admetSAR 3.0 predicted very

low Caco-2 permeability (Caco-2 probability 0.003; logPapp -6.55), a low probability of human intestinal absorption (HIA = 0.085), and a high probability of cobalamin being a P-glycoprotein substrate (0.949), suggesting poor passive intestinal permeability and a propensity for efflux transport. For distribution, both tools supported a moderate apparent volume of distribution (VDss ~0.3-0.5 L/kg) and high plasma protein binding (approximately 75%). Regarding the blood-brain barrier, ADMETlab 3.0 yielded a BBB score of 0.000462, and admetSAR 3.0 predicted a blood brain barrier permeability probability of 0.06, both indicating that cobalamin is very unlikely to cross the blood brain barrier efficiently by passive diffusion. Overall, these in silico results consistently suggest that cobalamin exhibits poor passive permeability (including across the blood brain barrier), together with a moderate distribution volume and substantial plasma protein binding.

#### **4. Discussion**

With the rapid development of the economy and society, the prevalence of ischemic stroke has gradually increased worldwide, leading to a heavy economic and social burden. Our previous clinical studies have identified cobalamin deficiency as a significant predictor of the occurrence and development of ischemic stroke, and early supplementation of cobalamin can improve patient outcomes (10-12). Additionally, cobalamin is a bioactive compound with multiple beneficial effects, including neuroprotective roles in ischemic stroke, such as epigenetic regulation, mitochondrial function modulation, and the preservation of the neurovascular unit integrity. A study involving 43,732 men without cardiovascular disease or diabetes found that vitamin B12 intake was negatively associated with ischemic stroke. Compared to the lowest intake group, the highest intake group had an adjusted multivariable hazard ratio of 0.73 (95% confidence interval: 0.53-0.99;  $P < 0.05$ ) (28). In another study, 224 patients with ischemic stroke and H-type hypertension received conventional treatment and were given 500  $\mu\text{g}$  of methylcobalamin daily for 6 months. The results showed that methylcobalamin

significantly reduced plasma tHcy and hs-CRP levels, decreased carotid intima-media thickness, and improved both NIHSS and BI scores, thereby effectively enhancing the patients' prognosis (29). In this study, we used network pharmacology, bioinformatics analysis, molecular docking simulations and MD simulations to explore potential therapeutic targets and mechanisms of cobalamin in ischemic stroke from multiple perspectives. The aim of this study is to investigate the potential therapeutic targets of cobalamin in the treatment of ischemic stroke.

First, we identified and validated a set of target genes closely associated with ischemic stroke, including ALB, TIMP1, PLG, FN1, AGT, SERPINE1, APOE, and SPP1. These genes are critically involved in the pathophysiological processes of stroke, encompassing blood circulation, neuroprotection, inflammation, apoptosis, and vascular remodeling. Notably, our study demonstrated that cobalamin is predicted to interact with these genes, suggesting its potential therapeutic value in promoting neurological recovery following ischemic stroke.

ALB is the most abundant circulating protein in the bloodstream and plays a multifaceted biological role. Its functions include binding and transporting a wide array of plasma drugs and endogenous molecules, maintaining colloid osmotic pressure, and exerting antioxidant, anticoagulant, and antiplatelet effects (30-32). Previous studies have identified serum ALB levels as predictive biomarkers for both the occurrence of stroke and unfavorable outcomes following stroke. The PIVOTAL trial, which enrolled 2,141 participants, reported that lower ALB levels were independently associated with an increased risk of stroke over a median follow-up of 2.1 years, suggesting that ALB may be an important predictor of stroke risk in this population (33). Similarly, findings from the CNSR-III, which analyzed data from 13,618 patients with acute ischemic stroke or transient ischemic attack, demonstrated that reduced serum ALB was an independent predictor of poor prognosis. Patients with ALB levels <35 g/L had a 37% higher risk of

unfavorable functional outcomes at 3 months (adjusted OR = 1.37) and a 113% higher risk of mortality (adjusted HR = 2.13). Additionally, for every 10 g/L reduction in ALB, the risk of adverse outcomes further increased (OR = 1.17, HR = 1.86). These associations remained significant throughout the 1-year follow-up period, reinforcing the prognostic value of serum ALB in stroke patients (34). Collectively, these findings underscore the multifactorial role of ALB in ischemic stroke pathology-not only as a prognostic biomarker but also as a potential therapeutic target for redox modulation and hemodynamic stabilization. Cobalamin, known for its antioxidant properties, may enhance these effects via upregulation of ALB expression, providing a plausible neuroprotective mechanism (35).

TIMP1 is an endogenous inhibitor of matrix metalloproteinases (MMPs) and plays a crucial role in maintaining the integrity of the blood-brain barrier (36). A cohort study by Zhong et al. reported that elevated serum TIMP1 levels at admission were associated with poor outcomes in stroke patients (37). Existing evidence suggests that during acute brain injury, the endogenous expression of TIMP1 is insufficient to provide adequate neuroprotection, indicating the need for exogenous supplementation to achieve its full therapeutic potential. The neuroprotective mechanisms of TIMP1 may include: (1) inhibition of MMP-9-mediated blood-brain barrier disruption; (2) attenuation of inflammatory responses; and (3) promotion of tissue repair (37, 38). These findings support the rationale for developing TIMP1-targeted therapeutic strategies in stroke management. Thus, by promoting TIMP1 expression, cobalamin may contribute to maintaining blood-brain barrier integrity, suppressing neuroinflammation, and improving post-stroke recovery- a hypothesis worthy of further *in vivo* validation.

PLG, a core component of the fibrinolytic system, not only facilitates thrombolysis but also modulates stroke progression through its roles in resolving inflammation, regulating immune cell migration, and providing neuroprotection. Dysregulation of PLG function has been closely associated

with the onset and development of stroke (39). Similarly, genetic polymorphisms in SERPINE1, which also acts as a chemotactic factor, have been associated with an increased risk of ischemic stroke and may exacerbate neuronal injury after ischemia-reperfusion by enhancing neutrophil infiltration (40). Dysregulation of the coagulation-fibrinolysis axis may also contribute to cerebral hemorrhage by compromising vascular stability. For instance, polymorphisms in the FN1 gene-such as rs10202709-are significantly associated with the risk of intraventricular hemorrhage (IVH) in preterm infants, with carriers of the TT genotype being more prone to developing high-grade IVH (41). Moreover, elevated plasma levels of cellular fibronectin, a splice variant of FN1, have been identified as a biomarker for hemorrhagic transformation and poor clinical outcomes in patients with acute ischemic stroke (42). Collectively, these findings highlight the therapeutic relevance of modulating the fibrinolytic pathway in ischemic stroke. The observed regulatory effects of cobalamin on PLG and SERPINE1 expression suggest a potential for restoring hemostatic equilibrium and attenuating secondary brain injury. This supports the rationale for exploring cobalamin as a multi-target agent capable of simultaneously modulating thrombotic and inflammatory mechanisms post-stroke

The M235T polymorphism in the AGT gene has been significantly associated with an increased risk of ischemic stroke-particularly lacunar infarction in men-among Asian populations (43). The underlying mechanisms may involve impaired regulation of blood pressure and accelerated atherosclerotic progression. APOE also contributes to stroke susceptibility through epigenetic regulation: its DNA methylation status may modulate key pathways involved in atherogenesis (44), while APOE genotype variations may further elevate cardiovascular risk by disrupting fatty acid metabolism (45). SPP1 plays a critical role in orchestrating the inflammatory response during the acute phase of stroke. After cerebral ischemia-reperfusion injury, SPP1 expression is significantly upregulated and is negatively regulated by miR-340-5p,

highlighting its potential as a therapeutic target for anti-inflammatory strategies (46). SPP1<sup>+</sup> macrophages have been shown to promote stroke-associated inflammation following aneurysmal rupture by driving phenotypic switching of vascular smooth muscle cells and facilitating collagen remodeling (47). Furthermore, in the MCAO model, activation of SPP1<sup>+</sup> microglia exacerbates pontine infarction, whereas inhibiting their activity confers neuroprotective effects (48). Taken together, AGT, APOE, and SPP1 represent distinct but convergent pathways-hypertension, lipid metabolism, and inflammation-that underlie stroke pathogenesis. The observed regulatory effects of cobalamin on these targets suggest a multifactorial mechanism of neuroprotection, providing further justification for its exploration as a candidate therapeutic agent with pleiotropic effects in ischemic stroke.

KEGG enrichment analysis revealed that the complement and coagulation cascades, along with the PI3K/Akt signaling pathway, are closely associated with the pathogenesis of stroke. Cobalamin deficiency contributes to increased stroke risk through multiple mechanisms. On one hand, it leads to abnormal accumulation of blood cells in the bone marrow. The resulting fragility of erythrocyte membranes predisposes them to intramedullary hemolysis, causing erythrocyte fragmentation and thrombocytopenia. The accumulation of hemolytic byproducts further damages the vascular endothelium (49). On the other hand, cobalamin deficiency promotes the buildup of toxic metabolites such as homocysteine and methylmalonic acid, which impair endothelial function through oxidative stress. This triggers platelet activation and upregulation of tissue factor expression, ultimately initiating the coagulation cascade and exacerbating vascular pathology (50). The complement system exerts a dual role in ischemic stroke: while its activation aggravates cerebral ischemia/reperfusion injury and inflammatory responses, it also participates in neural repair processes. Clinical studies have shown that elevated levels of complement components, such as C3, are positively correlated with the degree of neurological impairment in patients with

ischemic stroke (51, 52), suggesting that the complement cascade may serve as a dynamic target for modulating both injury and repair mechanisms after stroke.

The PI3K/Akt pathway plays a central neuroprotective role in stroke by regulating cell proliferation, survival, and metabolism. In cerebral ischemia/reperfusion injury, activation of this pathway alleviates oxidative and endoplasmic reticulum stress, suppresses inflammation, neuronal apoptosis, autophagy, and pyroptosis, and preserves the integrity of the blood-brain barrier. These effects collectively contribute to a reduction in infarct volume and improvement in neurological function (53-55). Notably, cobalamin supplementation has been shown to activate the PI3K/Akt pathway, leading to increased expression of brain-derived neurotrophic factor, inhibition of neuronal apoptosis, and attenuation of neurological damage in cerebral palsy models (56), further underscoring the therapeutic potential of this signaling axis in stroke.

Through MD simulations and ADME analysis, this study highlights the potential of cobalamin in the treatment of ischemic stroke. The simulation results indicate that cobalamin demonstrates strong binding stability with key targets, such as ALB, TIMP1, and PLG, with the ALB-Cobalamin and TIMP1-Cobalamin complexes exhibiting low RMSD and high stability. These findings suggest that cobalamin may exert neuroprotective effects through multiple mechanisms, including antioxidant activity, preservation of blood-brain barrier integrity, and regulation of thrombus formation. However, ADME analysis reveals that cobalamin has a high molecular weight and polar surface area, which, coupled with its poor ability to cross the blood-brain barrier, may limit its efficacy as an oral drug. Nevertheless, due to its high plasma protein binding and stability, cobalamin shows promise as a co-therapeutic agent. Future studies should focus on validating these simulation results and exploring more effective delivery methods to fully realize the therapeutic potential of cobalamin in ischemic stroke treatment.

This study, through computational modeling, revealed that cobalamin may exert neuroprotective effects by modulating multiple key genes and signaling pathways, offering novel insights into the treatment of ischemic stroke. However, several limitations should be acknowledged. First, the findings rely on computational predictions, which have not yet been validated by *in vitro*, *in vivo*, or clinical studies. This means that while the potential interactions between cobalamin and key stroke-related genes are promising, they require further experimental validation. Second, this study did not include comparisons with existing stroke therapies or explore the potential of combination interventions, which could provide more context for the therapeutic potential of cobalamin. Additionally, the optimal therapeutic dosage of cobalamin remains undefined, and further studies are needed to determine this. Future research should focus on experimentally validating the identified targets and pathways, investigating their underlying mechanisms, and evaluating both the clinical efficacy and safety of cobalamin-based interventions. These efforts will be essential for advancing the translational potential of cobalamin in stroke therapy. Despite these limitations, the present study provides a valuable framework for further investigation into the mechanisms by which cobalamin may act in the treatment of stroke, representing an important contribution to the field.

## **5. Conclusion**

In this study, we employed a combination of network pharmacology, bioinformatics analysis, and molecular docking simulations to investigate the potential mechanisms of cobalamin in the treatment of ischemic stroke. Our findings indicate that cobalamin targets a broad range of molecules implicated in ischemic stroke, and its therapeutic effects may be mediated through the reversal of aberrant expression of key genes, including ALB, TIMP1, PLG, FN1, AGT, SERPINE1, APOE, and SPP1. Moreover, the complement and coagulation cascades, as well as the PI3K/Akt signaling pathway, emerged as potential therapeutic pathways. These findings provide a comprehensive understanding

of the molecular targets through which cobalamin may exert neuroprotective effects, offering a theoretical foundation for its clinical application in ischemic stroke treatment.

### **Abbreviations**

WHO = World Health Organization

rt-PA = Recombinant Tissue Plasminogen Activator

ALB = Albumin

TIMP1 = Tissue Inhibitor of Metalloproteinases 1

PLG = Plasminogen

FN1 = Fibronectin 1

AGT = Angiotensinogen

SERPINE1 = Serpin Family E Member 1

APOE = Apolipoprotein E

SPP1 = Secreted Phosphoprotein 1

PPI = Protein-Protein Interaction

GO = Gene Ontology

KEGG = Kyoto Encyclopedia of Genes and Genomes

FDR = False Discovery Rate

DAVID = Database for Annotation, Visualization, and Integrated Discovery

STRING = Search Tool for the Retrieval of Interacting Genes

MCC = Maximal Clique Centrality

BP = Biological Process

CC = Cellular Component

MF = Molecular Function

MCODE = Molecular Complex Detection

CytoNCA = Cytoscape Network Centrality Analysis

VWF = Von Willebrand Factor

CRP = C-Reactive Protein

PME = Particle Mesh Ewald

NVT = Number of particles (N), Volume (V), and Temperature (T) ensemble  
NPT = Number of particles (N), Pressure (P), and Temperature (T) ensemble  
ADMET = Absorption, Distribution, Metabolism, Excretion, and Toxicity  
BBB = Blood-Brain Barrier  
TPSA = Topological Polar Surface Area  
HIA = Human Intestinal Absorption  
CGenFF = CHARMM General Force Field  
RMSD = Root Mean Square Deviation  
RMSF = Root Mean Square Fluctuation  
Rg = Radius of Gyration  
SASA = Solvent Accessible Surface Area  
MD = Molecular Dynamics  
PDB = Protein Data Bank  
MCC = Maximal Clique Centrality  
MCAO = Middle Cerebral Artery Occlusion  
tHcy = Total Homocysteine  
hs-CRP = High-Sensitivity C-Reactive Protein

### **Acknowledgments**

We thank all investigators contributed to this article. We also give thanks to all patients enrolled in this study.

### **Data Availability**

All data analysed during this study are included in the websites mentioned above. The mass spectrometry proteomics data have been deposited to the ProteomeXchange Consortium (<http://proteomecentral.proteomexchange.org>) via the PRIDE partner repository (57) with the dataset identifier PXD062264. The data not published within this article are available from the corresponding author on reasonable request.

### **Funding**

This work was supported by the National Natural Science Foundation of

China (Grant No. 82171456) awarded to Qin Yang and the 2023 Research Planning Project of the Sichuan Provincial Psychological Society (No. SCSXLXH2023034) awarded to Pingping Liu.

### **Author contributions**

Q.Y. contributed to the study conception and design and provided critical revisions and editorial input for the manuscript. L. Z. and Y.C. jointly drafted the initial version of the manuscript and developed the primary tables and figures. H.W. and J.W. performed the data analysis. F.X. and P.L. were responsible for data acquisition from the relevant datasets. All authors were involved in the study design, contributed to manuscript revisions, and approved the final version of the manuscript.

### **Declarations**

#### **Ethics approval and consent to participate**

Not applicable.

#### **Consent for publication**

Not applicable.

#### **Competing interests**

The authors have no competing interests to declare.

### **Reference**

- [1] Qin C, Dong M, Tang Y, et al. The foam cell-derived exosomal miRNA Novel-3 drives neuroinflammation and ferroptosis during ischemic stroke. *Nat Aging*. 2024;4(12):1845-1861.
- [2] Qin C, Yang S, Chu Y, et al. Signaling pathways involved in ischemic stroke: molecular mechanisms and therapeutic interventions. *Signal Transduct Target Ther*. 2022;7(1):215.
- [3] GBD 2019 Stroke Collaborators. Global, regional, and national burden of stroke and its risk factors, 1990-2019: a systematic analysis for the Global Burden of Disease Study 2019. *Lancet Neurol*. 2021;20(10):795-820.
- [4] Roth W, Mohamadzadeh M. Vitamin B12 and gut-brain homeostasis in the pathophysiology of ischemic stroke. *EBioMedicine*. 2021;73:103676.
- [5] Sands T, Jawed A, Stevenson E, Smith M, Jawaid I. Vitamin B12 deficiency: NICE guideline summary. *BMJ*. 2024;385:q1019.

- [6] Zhou L, Song X, Wang J, Tan Y, Yang Q. Effects of vitamin B12 deficiency on risk and outcome of ischemic stroke. *Clin Biochem.* 2023;118:110591.
- [7] Mitra S, Natarajan R, Ziedonis D, Fan X. Antioxidant and anti-inflammatory nutrient status, supplementation, and mechanisms in patients with schizophrenia. *Prog Neuropsychopharmacol Biol Psychiatry.* 2017;78:1-11.
- [8] Li Z, Xue B, Jiagui H, Yongjun T, Qin Y. Vitamin B12 supplementation improves cognitive function in middle aged and elderly patients with cognitive impairment. *Nutr Hosp.* 2023;40(4):762-769.
- [9] Reynolds EH. Vitamin B12, folic acid, and the nervous system. *Lancet Neurol.* 2006;5(11):949-960.
- [10] Zhou L, Wang J, Li M, et al. Low vitamin B12 levels may predict the risk of ischemic stroke: A cross-sectional study. *J Clin Neurosci.* 2023;117:125-135.
- [11] Chen X, Yu P, Zhou L, et al. Low concentration of serum vitamin B12 may be a strong predictor of large-artery atherosclerosis stroke: A case-control study. *Clin Biochem.* 2024;131-132:110813.
- [12] Zhou L, Wang J, Wu H, et al. Serum levels of vitamin B12 combined with folate and plasma total homocysteine predict ischemic stroke disease: a retrospective case-control study. *Nutr J.* 2024;23(1):76.
- [13] Nogales C, Mamdouh Z, List M, et al. Network pharmacology: curing causal mechanisms instead of treating symptoms. *Trends Pharmacol Sci.* 2022;43(2):136-150.
- [14] Safran M, Dalah I, Alexander J, et al. GeneCards Version 3: the human gene integrator. *Database (Oxford).* 2010;2010:baq020.
- [15] Knox C, Wilson M, Klinger CM, et al. DrugBank 6.0: the DrugBank Knowledgebase for 2024. *Nucleic Acids Res.* 2024;52(D1):D1265-D1275.
- [16] Mi H, Ebert D, Muruganujan A, et al. PANTHER version 16: a revised family classification, tree-based classification tool, enhancer regions and extensive API. *Nucleic Acids Res.* 2021;49(D1):D394-D403.
- [17] Kanehisa M, Furumichi M, Sato Y, Matsuura Y, Ishiguro-Watanabe M. KEGG: biological systems database as a model of the real world. *Nucleic Acids Res.* 2025;53(D1):D672-D677.
- [18] Kanehisa M. Toward understanding the origin and evolution of cellular organisms. *Protein Sci.* 2019;28(11):1947-1951.
- [19] Kanehisa M, Goto S. KEGG: Kyoto encyclopedia of genes and genomes. *Nucleic Acids Res.* 2000;28(1):27-30.
- [20] Dennis G, Sherman BT, Hosack DA, et al. DAVID: Database for Annotation, Visualization, and Integrated Discovery. *Genome Biol.* 2003;4(5):P3.
- [21] Jiménez-García N, de la Torre Lima J, García Alegría J. The role of aspirin

as antiaggregant therapy in primary prevention. An update. *Med Clin (Barc)*. 2019;153(8):326-331.

[22] Trott O, Olson AJ. AutoDock Vina: improving the speed and accuracy of docking with a new scoring function, efficient optimization, and multithreading. *J Comput Chem*. 2010;31(2):455-461.

[23] Mooers BHM, Brown ME. Templates for writing PyMOL scripts. *Protein Sci*. 2021;30(1):262-269.

[24] Sanner MF. Python: a programming language for software integration and development. *J Mol Graph Model*. 1999;17(1):57-61.

[25] Shannon P, Markiel A, Ozier O, et al. Cytoscape: a software environment for integrated models of biomolecular interaction networks. *Genome Res*. 2003;13(11):2498-2504.

[26] Sherman BT, Hao M, Qiu J, et al. DAVID: a web server for functional enrichment analysis and functional annotation of gene lists (2021 update). *Nucleic Acids Res*. 2022;50(W1):W216-W221.

[27] Piñero J, Ramírez-Anguaita JM, Saüch-Pitarch J, et al. The DisGeNET knowledge platform for disease genomics: 2019 update. *Nucleic Acids Res*. 2020;48(D1):D845-D855.

[28] Wishart DS, Knox C, Guo AC, et al. DrugBank: a knowledgebase for drugs, drug actions and drug targets. *Nucleic Acids Res*. 2008;36(Database issue):D901-D906.

[29] Amberger JS, Bocchini CA, Schiettecatte F, Scott AF, Hamosh A. OMIM.org: Online Mendelian Inheritance in Man (OMIM®), an online catalog of human genes and genetic disorders. *Nucleic Acids Res*. 2015;43(Database issue):D789-D798.

[30] Seeliger D, de Groot BL. Ligand docking and binding site analysis with PyMOL and Autodock/Vina. *J Comput Aided Mol Des*. 2010;24(5):417-422.

[31] Tian W, Chen C, Lei X, Zhao J, Liang J. CASTp 3.0: computed atlas of surface topography of proteins. *Nucleic Acids Res*. 2018;46(W1):W363-W367.

[32] Szklarczyk D, Kirsch R, Koutrouli M, et al. The STRING database in 2023: protein-protein association networks and functional enrichment analyses for any sequenced genome of interest. *Nucleic Acids Res*. 2023;51(D1):D638-D646.

[33] Daina A, Michielin O, Zoete V. SwissTargetPrediction: updated data and new features for efficient prediction of protein targets of small molecules. *Nucleic Acids Res*. 2019;47(W1):W357-W364.

[34] UniProt Consortium. UniProt: the universal protein knowledgebase in 2023. *Nucleic Acids Res*. 2023;51(D1):D523-D531.

- [35] Dong J, Wang N, Yao Z, et al. ADMETlab: a platform for systematic ADMET evaluation based on a comprehensively collected ADMET database. *J Cheminform.* 2018;10(1):29.
- [36] Yang H, Lou C, Sun L, et al. admetSAR 2.0: web-service for prediction and optimization of chemical ADMET properties. *Bioinformatics.* 2019;35(6):1067-1069.
- [37] Cheng F, Li W, Zhou Y, et al. admetSAR: a comprehensive source and free tool for assessment of chemical ADMET properties. *J Chem Inf Model.* 2012;52(11):3099-3105.
- [38] Yang H, Lou C, Sun L, et al. admetSAR 2.0: web-service for prediction and optimization of chemical ADMET properties. *Bioinformatics,* 2019, 35(6), 1067-1069.
- [39] Vanommeslaeghe K, Hatcher E, Acharya C, et al. CHARMM general force field: A force field for drug-like molecules compatible with the CHARMM all-atom additive biological force fields. *J Comput Chem.* 2010;31(4):671-690.
- [40] Dolezal R, Soukup O, Malinak D, et al. Towards understanding the mechanism of action of antibacterial N-alkyl-3-hydroxypyridinium salts: Biological activities, molecular modeling and QSAR studies. *Eur J Med Chem.* 2016;121:699-711.
- [41] Childers MC, Daggett V. Validating Molecular Dynamics Simulations against Experimental Observables in Light of Underlying Conformational Ensembles. *J Phys Chem B.* 2018;122(26):6673-6689.
- [42] He K, Merchant A, Rimm EB, et al. Folate, vitamin B6, and B12 intakes in relation to risk of stroke among men. *Stroke.* 2003;35(1):169-174.
- [43] Yuan M, Wang B, Tan S. Mecobalamin and early functional outcomes of ischemic stroke patients with H-type hypertension. *Rev Assoc Med Bras (1992).* 2018;64(5):428-432.
- [44] Zoanni B, Brioschi M, Mallia A, et al. Novel insights about albumin in cardiovascular diseases: Focus on heart failure. *Mass Spectrom Rev.* 2023;42(4):1113-1128.
- [45] Lam FW, Cruz MA, Leung HC, et al. Histone induced platelet aggregation is inhibited by normal albumin. *Thromb Res.* 2013;132(1):69-76.
- [46] Paar M, Rossmann C, Nussold C, et al. Anticoagulant action of low, physiologic, and high albumin levels in whole blood. *PLoS One.* 2017;12(8):e0182997.
- [47] Mark PB, Jhund PS, Walters MR, et al. Stroke in Hemodialysis Patients Randomized to Different Intravenous Iron Strategies: A Prespecified Analysis from the PIVOTAL Trial. *Kidney360.* 2021;2(11):1761-1769.

- [48] Zhou H, Wang A, Meng X, et al. Low serum albumin levels predict poor outcome in patients with acute ischaemic stroke or transient ischaemic attack. *Stroke Vasc Neurol*. 2021;6(3):458-466.
- [49] Abu-Zahab ZA, Qureshi H, Adham GM, et al. Frequency of comorbid diseases with high serum Vitamin B12 levels in patients attending King Salman Medical City (KSAMC), at Madinah. *Int J Health Sci (Qassim)*. 2025;19(1):15-21.
- [50] Liu M, Wang W, Gao J, et al. Icariside II attenuates cerebral ischemia/reperfusion-induced blood-brain barrier dysfunction in rats via regulating the balance of MMP9/TIMP1. *Acta Pharmacol Sin*. 2020;41(12):1547-1556.
- [51] Zhong C, Wang G, Xu T, et al. Tissue inhibitor metalloproteinase-1 and clinical outcomes after acute ischemic stroke. *Neurology*. 2019;93(18):e1675-e1685.
- [52] Ries C. Cytokine functions of TIMP-1. *Cell Mol Life Sci*. 2014;71(4):659-672.
- [53] Perucci LO, Vago JP, Miles LA, Sousa LP. Crosstalk between the plasminogen/plasmin system and inflammation resolution. *J Thromb Haemost*. 2023;21(10):2666-2678.
- [54] Pu Z, Bao X, Xia S, Shao P, Xu Y. Serpine1 regulates peripheral neutrophil recruitment and acts as potential target in ischemic stroke. *J Inflamm Res*. 2022;15:2649-2663.
- [55] Szpecht D, Al-Saad SR, Karbowski LM, et al. Role of Fibronectin-1 polymorphism genes with the pathogenesis of intraventricular hemorrhage in preterm infants. *Childs Nerv Syst*. 2020;36(8):1729-1736.
- [56] Wang L, Deng L, Yuan R, et al. Association of Matrix Metalloproteinase 9 and Cellular Fibronectin and Outcome in Acute Ischemic Stroke: A Systematic Review and Meta-Analysis. *Front Neurol*. 2020;11:523506.
- [57] Wang S, Zeng R, Lei L, Huang J. Angiotensinogen gene polymorphism and ischemic stroke in East Asians: A meta-analysis. *Neural Regen Res*. 2013;8(13):1228-1235.
- [58] Kanehisa M, Furumichi M, Sato Y, Ishiguro-Watanabe M, Tanabe M. KEGG: integrating viruses and cellular organisms. *Nucleic Acids Res*. 2021;49(D1):D545-D51.
- [59] Qin X, Li J, Wu T, et al. Overall and sex-specific associations between methylation of the ABCG1 and APOE genes and ischemic stroke or other atherosclerosis-related traits in a sibling study of Chinese population. *Clin Epigenetics*. 2019;11(1):189.

- [60] Satizabal CL, Samieri C, Davis-Plourde KL, et al. APOE and the Association of Fatty Acids With the Risk of Stroke, Coronary Heart Disease, and Mortality. *Stroke*. 2018;49(12):2822-2829.
- [61] Nie Q, Zheng Z, Liao J, et al. SPP1/AnxA1/TIMP1 as essential genes regulate the inflammatory response in the acute phase of cerebral ischemia-reperfusion in rats. *J Inflamm Res*. 2022;15:4873-4890.
- [62] Lan Y, Zhang X, Liu S, et al. Fate mapping of Spp1 expression reveals age-dependent plasticity of disease-associated microglia-like cells after brain injury. *Immunity*. 2024;57(2):291-307.
- [63] Luo M, Qiu Z, Tang X, et al. Inhibiting Cyclin B1-treated Pontine Infarction by Suppressing Proliferation of SPP1+ Microglia. *Mol Neurobiol*. 2023;60(4):1782-1796.
- [64] Morrissey D, Sun Y, Koilpillai S, Kropf J, Carlan S. Pseudo-Thrombotic Microangiopathy Secondary to Vitamin B12 Deficiency. *Case Rep Med*. 2022;2022:7306070.
- [65] Lentz SR. Mechanisms of thrombosis in hyperhomocysteinemia. *Curr Opin Hematol*. 1998;5(5):343-349.
- [66] Ma Y, Liu Y, Zhang Z, Yang G. Significance of Complement System in Ischemic Stroke: A Comprehensive Review. *Aging Dis*. 2019;10(2):429-462.
- [67] Yang P, Zhu Z, Zang Y, et al. Increased Serum Complement C3 Levels Are Associated With Adverse Clinical Outcomes After Ischemic Stroke. *Stroke*. 2021;52(3):868-877.
- [68] Zhu B, Zhou X. [The study of PI3K/AKT pathway in lung cancer metastasis and drug resistance]. *Zhongguo Fei Ai Za Zhi*. 2011;14(8):689-694.
- [69] Han Y, Sun Y, Peng S, et al. PI3K/AKT pathway: A potential therapeutic target in cerebral ischemia-reperfusion injury. *Eur J Pharmacol*. 2025;998:177505.
- [70] Khan H, Singh A, Singh Y, et al. Pharmacological modulation of PI3K/PTEN/Akt/mTOR/ERK signaling pathways in ischemic injury: a mechanistic perspective. *Metab Brain Dis*. 2025;40(3):131-149.
- [71] Li E, Zhao P, Jian J, et al. Vitamin B1 and B12 mitigates neuron apoptosis in cerebral palsy by augmenting BDNF expression through MALAT1/miR-1 axis. *Cell Cycle*. 2019;18(21):2849-2859.
- [72] Perez-Riverol Y, Bandla C, Kundu DJ, et al. The PRIDE database at 20 years: 2025 update. *Nucleic Acids Res*. 2025;53(D1):D543-D553.

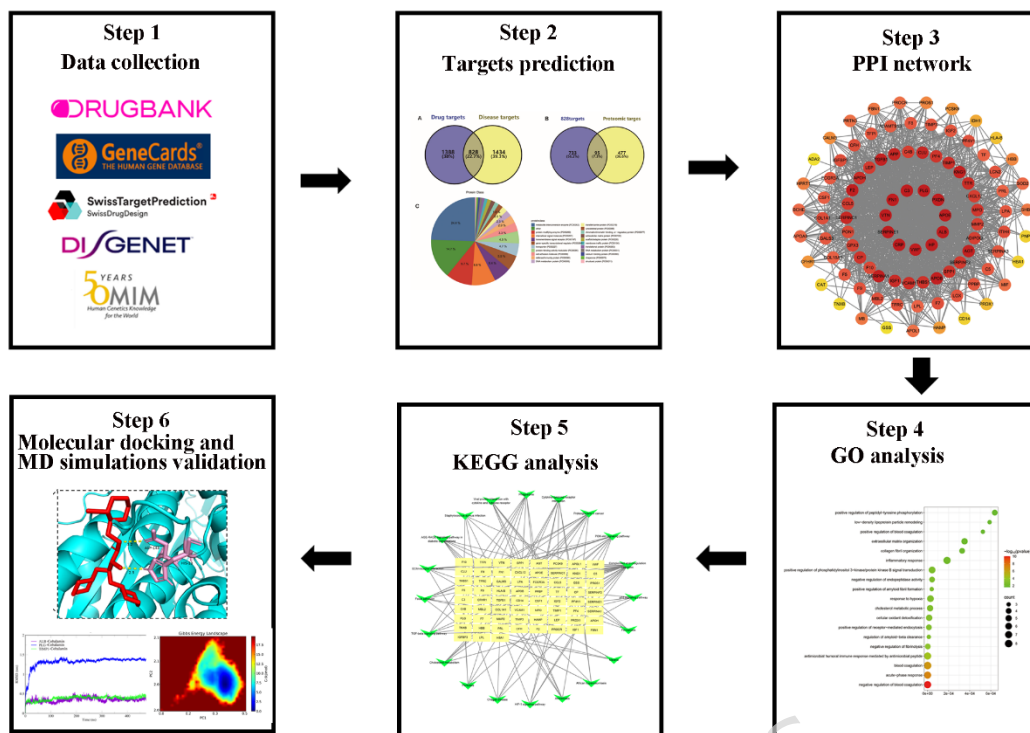


**Figure 1. A flowchart of the network pharmacology analysis used in the study**

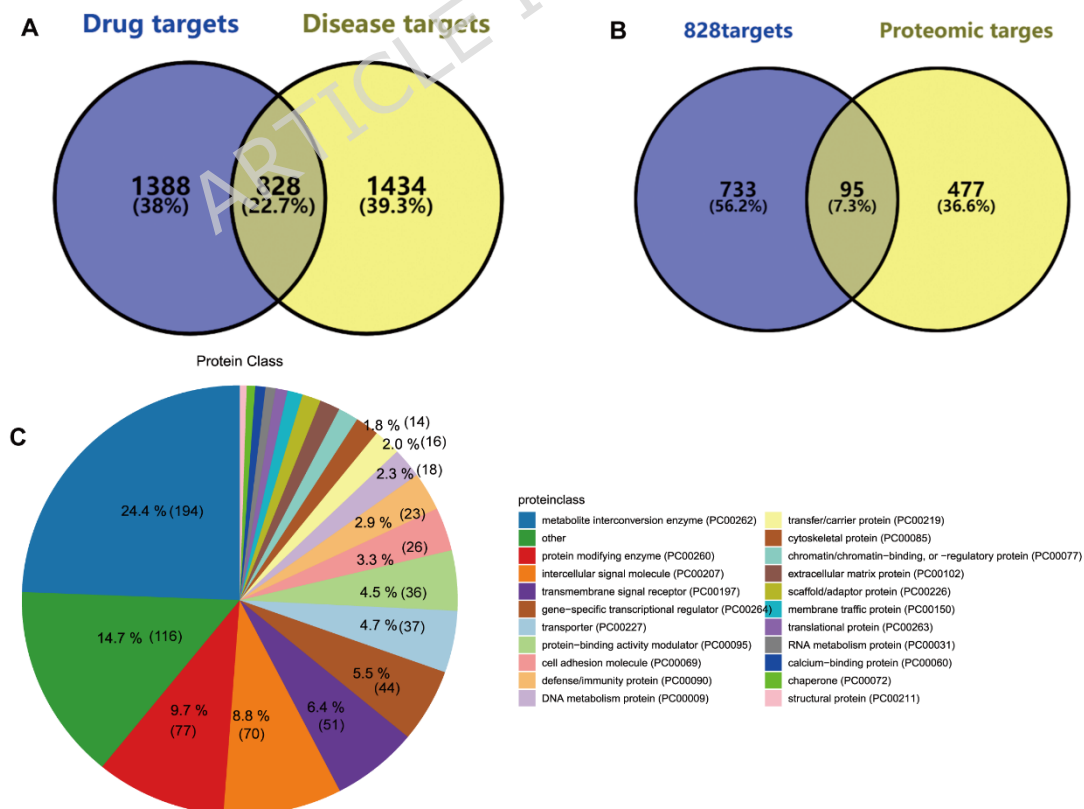


**Figure 2. Identification of genes regulating ischemic stroke by**

**cobalamin.** (A) The common targets of cobalamin and ischemic stroke. (B) The common targets between proteomic targets-cobalamin and ischemic stroke targets. (C) Classification of the identified targets.

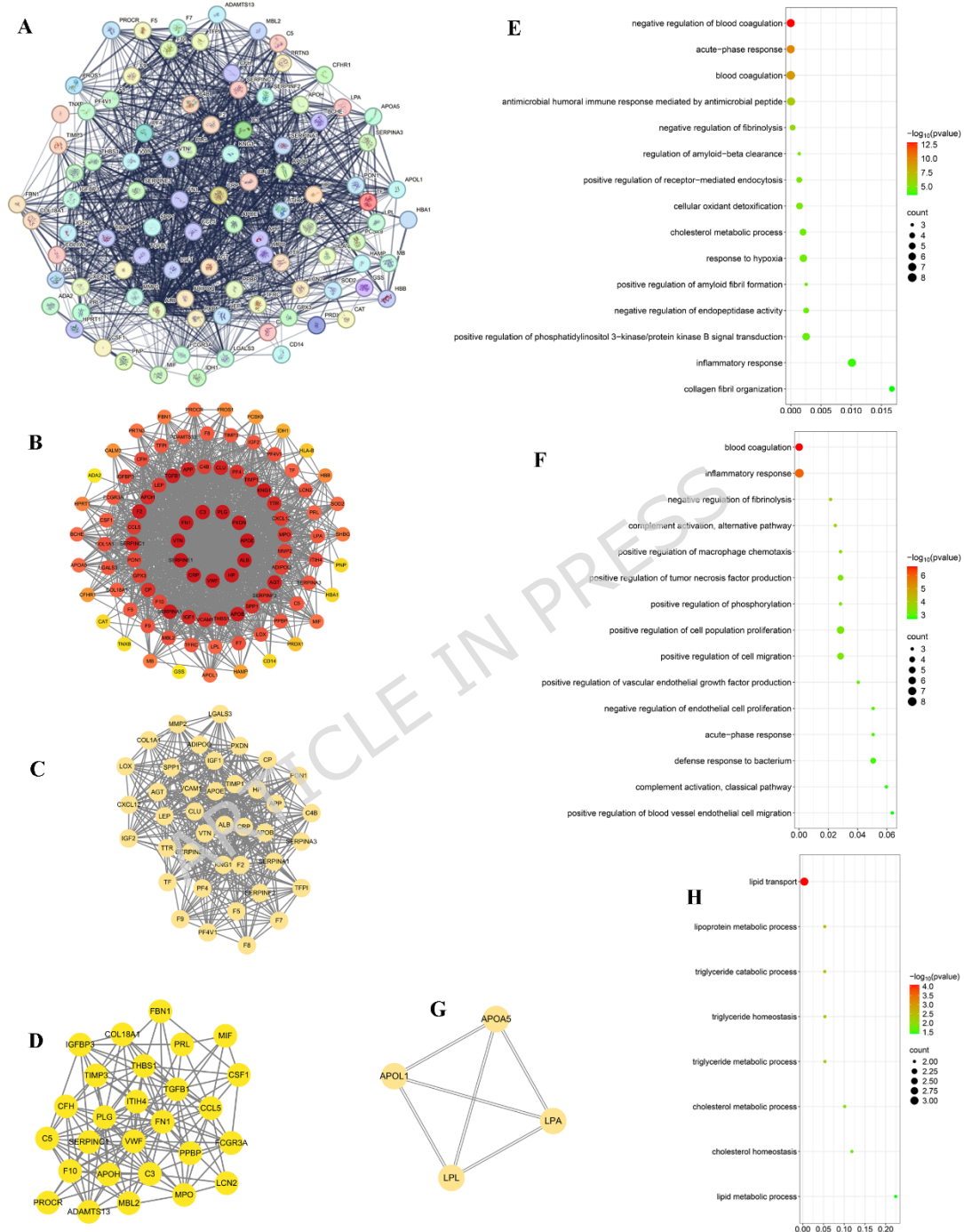


**Figure 3. The enrichment analysis of PPI network.** (A) The PPI network from STRING. (B) The visualization of PPI network. (C) The Cluster1 of PPI. (D) The Cluster2 of PPI. (E) The GO-BP analysis of Cluster1. (F) The GO-BP analysis of Cluster2. (G) The Cluster3 of PPI. (H) The GO-BP analysis of

## Cluster3.

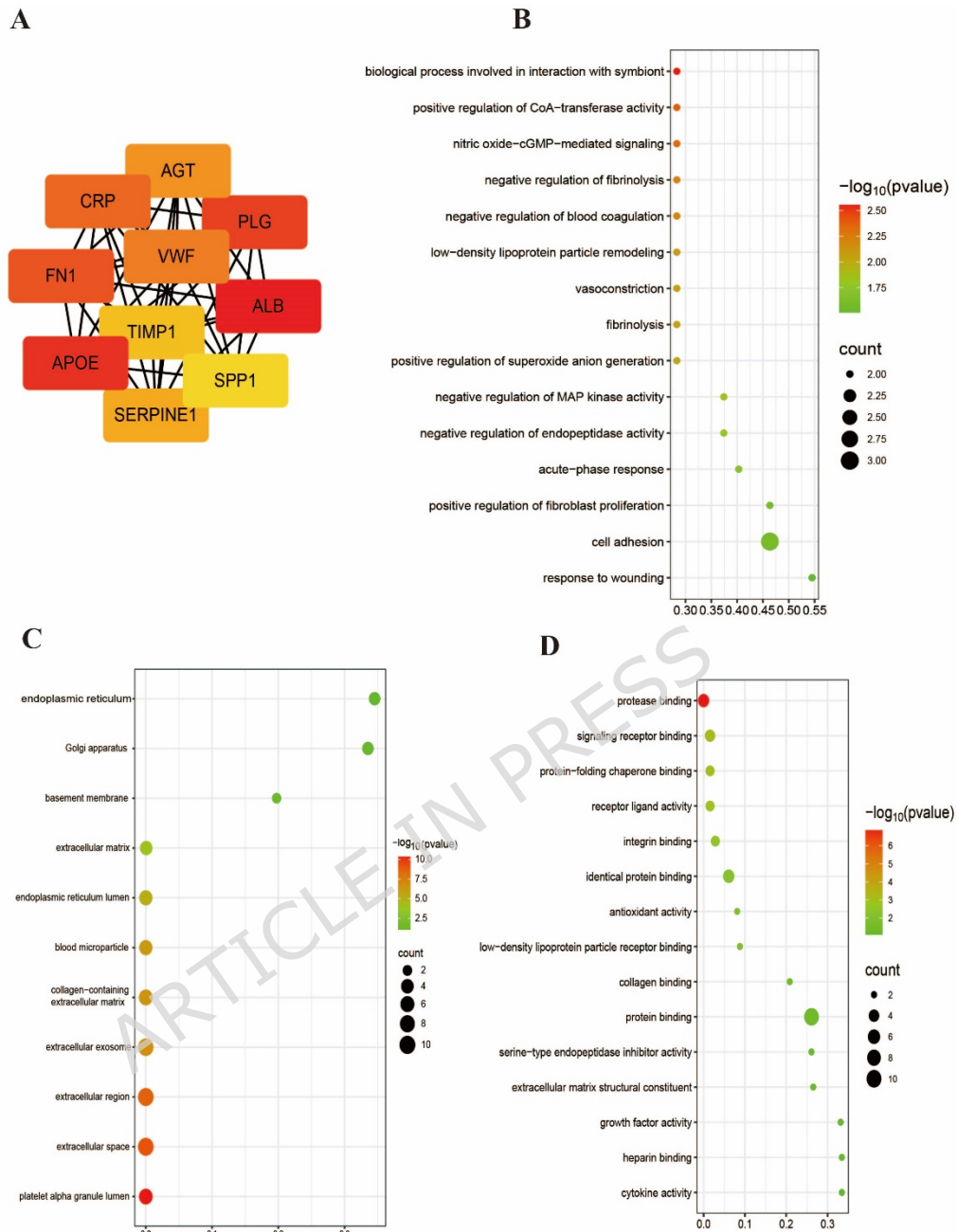


**Figure 4. The GO function enrichment analysis of core targets of cobalamin regulating ischemic stroke.** (A) The hub genes of PPI network. (B) The BP analysis of hub genes. (C) The CC analysis of hub genes. (D) The MF analysis of hub genes.

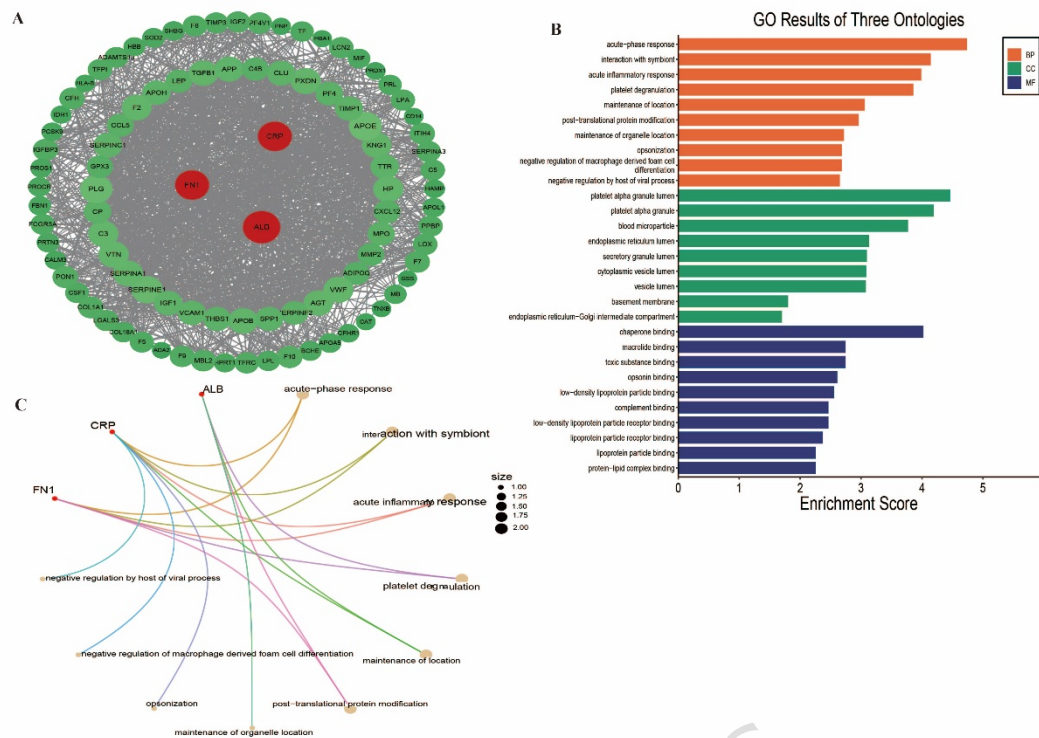


**Figure 5. The GO function enrichment analysis of core targets of cobalamin regulating ischemic stroke. (A) The hub genes of PPI network. (B) The BP, CC and MF analysis of hub genes. (C) The c-net analysis of hub genes.**

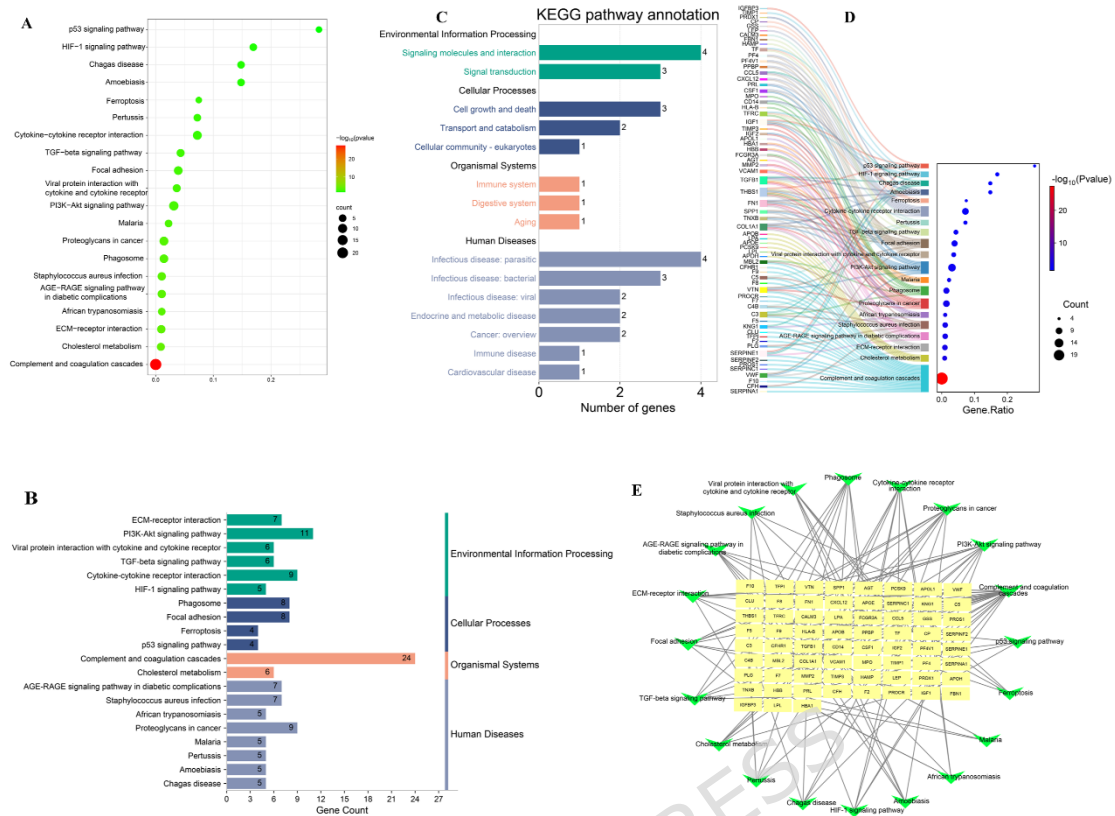


**Figure 6. The KEGG enrichment analysis identified the core pathways of cobalamin regulating ischemic stroke. (A)** KEGG pathway analysis. **(B)** KEGG classification analysis. **(C)** KEGG pathway annotation analysis. **(D)** The network of targets-pathways (Note: the V shape represents-pathway, the yellow rectangle represents target). **(E)** A pathway-target network, with green nodes representing signaling pathways and yellow nodes indicating target genes. Data from KEGG (58), available at [www.kegg.jp/kegg/kegg1.html](http://www.kegg.jp/kegg/kegg1.html).

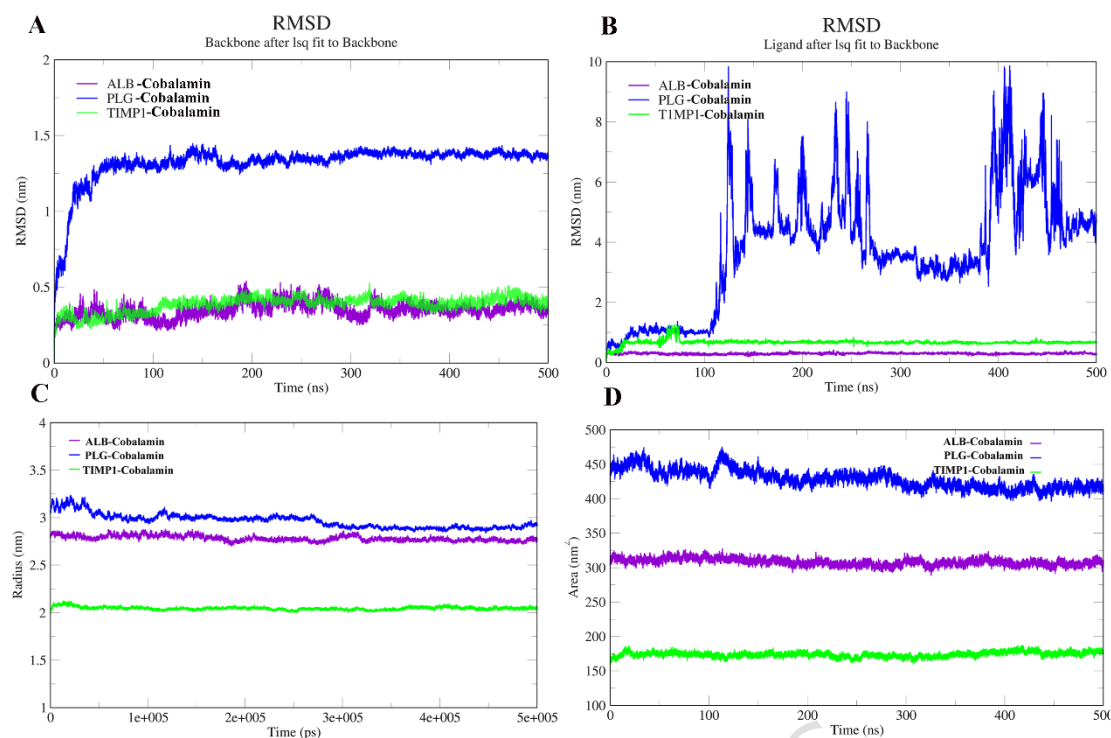


**Figure 7. RMSD, Radius of Gyration (Rg), and SASA Analysis of Protein-Cobalamin Complexes.** (A) Backbone RMSD (after least-squares fitting to backbone) for ALB-Cobalamin, PLG-Cobalamin, and TIMPI-Cobalamin complexes. (B) Ligand RMSD after backbone fitting, showing the stability of Cobalamin in the binding pockets. (C) Radius of Gyration (Rg) for the complexes. (D) Solvent Accessible Surface Area (SASA) analysis.

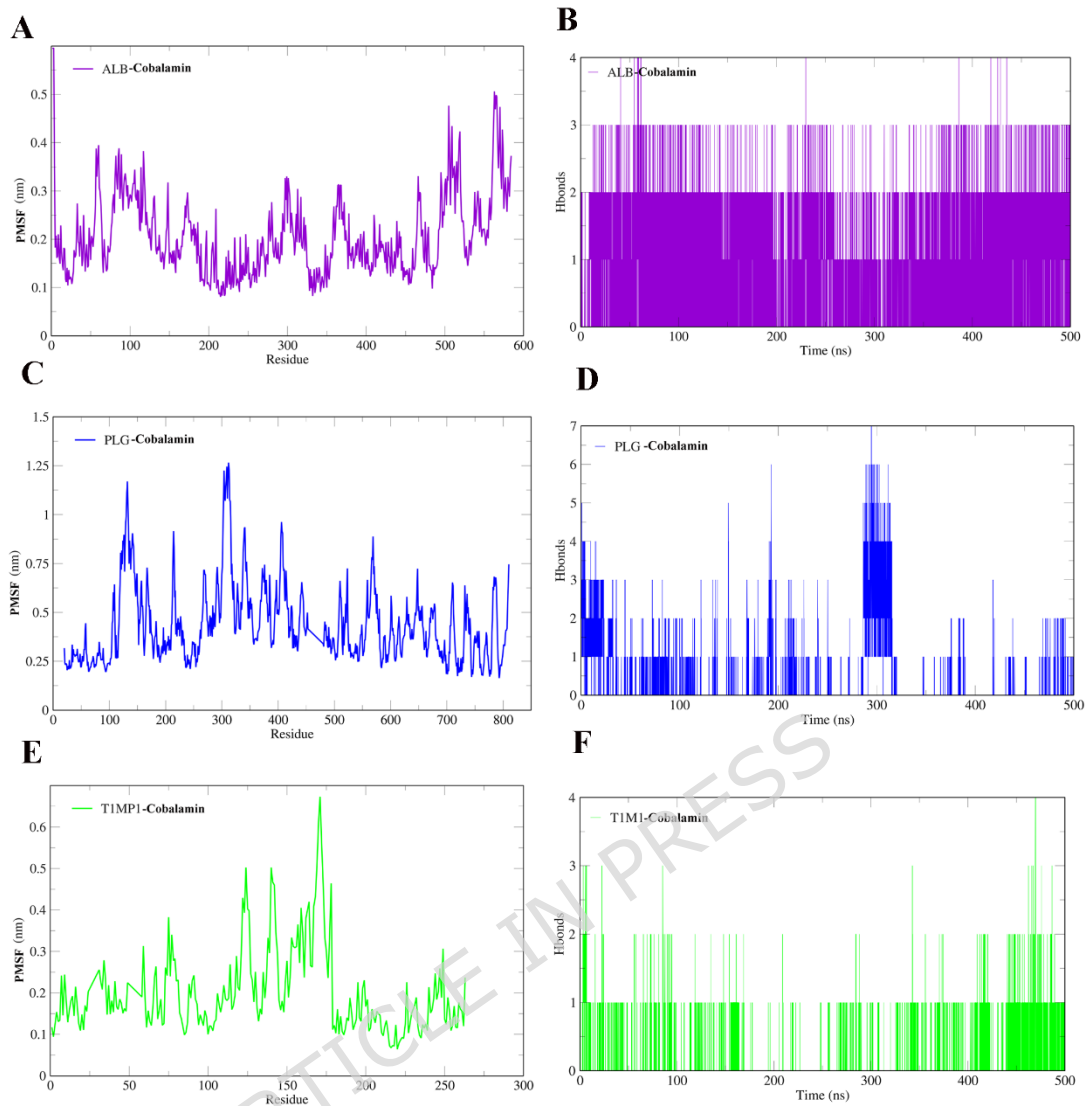


**Figure 8. RMSF and Hydrogen Bonding Analysis of Protein-Cobalamin Complexes.**

(A) RMSF of ALB-Cobalamin. (B) Hydrogen bonds in ALB-Cobalamin. (C) RMSF of PLG-Cobalamin. (D) Hydrogen bonds in PLG-Cobalamin. (E) RMSF of TIMPI-Cobalamin. (F) Hydrogen bonds in TIMPI-Cobalamin.

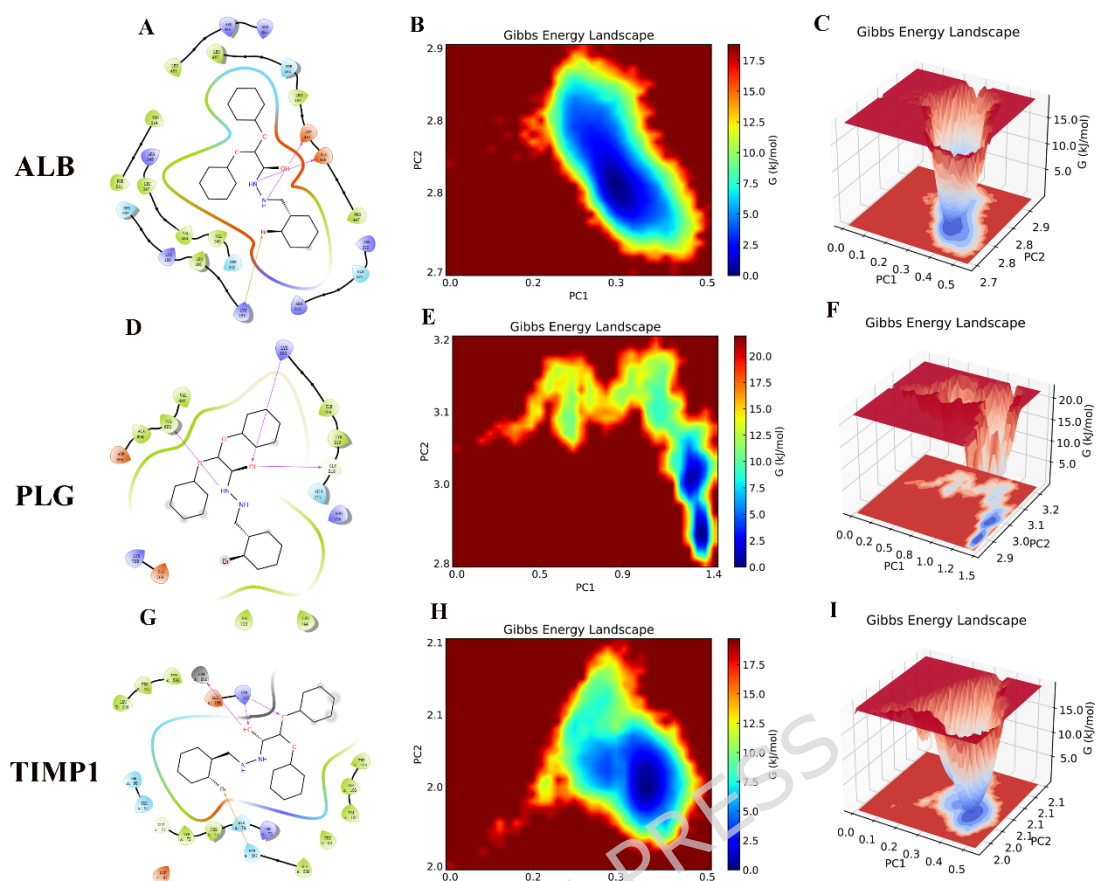


**Figure 9. Gibbs Free Energy Landscape of Protein-Cobalamin Complexes.** (A) Gibbs free energy landscape of ALB-Cobalamin. (B) Three-dimensional Gibbs free energy landscape of ALB-Cobalamin. (C) Three-dimensional Gibbs free energy plot of ALB-Cobalamin. (D) Gibbs free energy landscape of PLG-Cobalamin. (E) Three-dimensional Gibbs free energy landscape of PLG-Cobalamin. (F) Three-dimensional plot of PLG-Cobalamin's free energy. (G) Gibbs free energy landscape of TIMPI-Cobalamin. (H) Three-dimensional Gibbs free energy landscape of TIMPI-Cobalamin. (I) Three-dimensional Gibbs free energy plot of TIMPI-Cobalamin.

**Table 1. The webservers/software used in the study**

N	Database	Website	Versio	Referenc
O	and		n	es
	analysis			
	platform			

1	AutoDock Vina_v1.2.2	<a href="https://vina.scripps.edu/">https://vina.scripps.edu/</a>	V1.2.2	[19]
2	AutoDockTools	<a href="https://autodock.scripps.edu/resources/adt/">https://autodock.scripps.edu/resources/adt/</a>	V1.5.7	(59)
3	Cytoscape	<a href="https://cytoscape.org/">https://cytoscape.org/</a>	V3.10.1	(60)
4	DAVID Bioinformatics	<a href="https://david.ncifcrf.gov/tools.jsp">https://david.ncifcrf.gov/tools.jsp</a>	-	(61)
5	Draw Venn Diagram	<a href="http://bioinformatics.psb.ugent.be/webtools/Venn/">http://bioinformatics.psb.ugent.be/webtools/Venn/</a>	-	-
6	DisGeNet database	<a href="https://www.disgenet.org/">https://www.disgenet.org/</a>	-	(62)
7	Drugbank database	<a href="https://go.drugbank.com/">https://go.drugbank.com/</a>	V6.0	(63)
8	GeneCards database	<a href="https://www.genecards.org/">https://www.genecards.org/</a>	-	(14)
9	OMIM	<a href="https://omim.org/">https://omim.org/</a>	-	(64)
10	PubChem database	<a href="https://pubchem.ncbi.nlm.nih.gov/">https://pubchem.ncbi.nlm.nih.gov/</a>	-	-
11	Pymol	<a href="https://www.pymol.org/">https://www.pymol.org/</a>	V3.0.4	(65)
12	CASTp 3.0	<a href="http://sts.bioe.uic.edu/castp/">http://sts.bioe.uic.edu/castp/</a>	-	(66)
13	String tool	<a href="https://string-db.org/">https://string-db.org/</a>	V12.0	(67)
14	Swiss Target Prediction	<a href="http://www.swisstargetprediction.ch/">http://www.swisstargetprediction.ch/</a>	-	(68)
15	Uniprot database	<a href="https://www.uniprot.org/">https://www.uniprot.org/</a>	-	(69)
16	ADMETlab 3.0	<a href="https://admetlab3.scbdd.com/server/screening/">https://admetlab3.scbdd.com/server/screening/</a>	V3.0	(70)

17	admetSAR	<a href="https://lmmd.ecust.edu.cn/admetSar3/resour">https://lmmd.ecust.edu.cn/admetSar3/resour</a>	-	(71, 72)
	3.0	ce.php/		

**Table 2. The evaluation of drug-likeness properties on key metabolites**

NO.	Target	DC value	NO.	Target	DC value
1	ALB	37	20	F2	27
2	APOE	36	21	LEP	27
3	CRP	35	22	MPO	26
4	FN1	35	23	SPP1	26
5	PLG	35	24	CLU	25
6	VWF	32	25	TTR	25
7	VTN	32	26	PF4	25
8	APOB	32	27	PXDN	25
9	C3	31	28	ADIPOQ	24
10	AGT	31	29	APOH	24
11	SERPINE1	30	30	THBS1	23
12	KNG1	30	31	SERPINC1	23
13	APP	29	32	CCL5	22
14	TIMP1	29	33	CP	22
15	HP	29	34	PON1	21
16	TGFB1	28	35	C4B	21
17	SERPINA1	28	36	SERPINF2	20
18	VCAM1	28	37	MMP2	20
19	IGF1	27			

**Table 3. Molecular docking results of Cobalamin with target proteins**

<b>Drug</b>	<b>Targets</b>	<b>PDB ID</b>	<b>Energy (kcal/mol)</b>	<b>Full Fitness (kcal/mol)</b>	<b><math>\Delta G_{vdw}</math> (kcal/mol)</b>
Cobalamin	AGT	5M3X	-6.5	-4.5	-5.5
Cobalamin	ALB	6JE7	-8.7	-6.5	-7.4
Cobalamin	APOE	6V7M	-6.3	-4.2	-5.4
Cobalamin	FN1	4GH7	-6.8	-4.8	-5.8
Cobalamin	PLG	8UQ6	-7.9	-6	-6.7
Cobalamin	SERPINE1	9PAI	-6.5	-4.7	-5.5
Cobalamin	SPP1	3DSF	-6.2	-4.5	-5.3
Cobalamin	TIMP1	3V96	-8.2	-6.1	-7

ARTICLE IN PRESS

### Step 1 Data collection

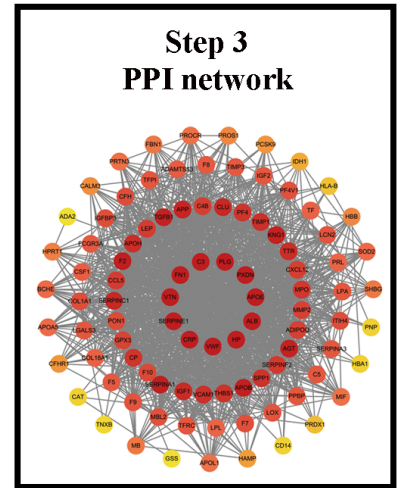


### Step 2 Targets prediction

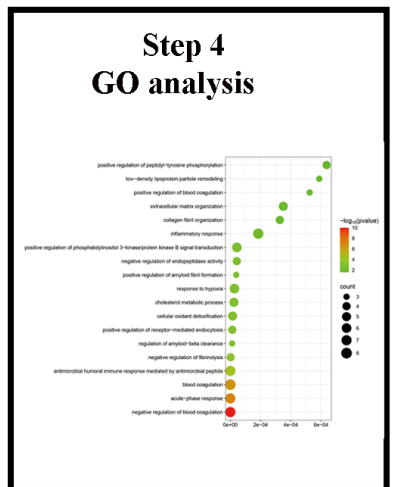
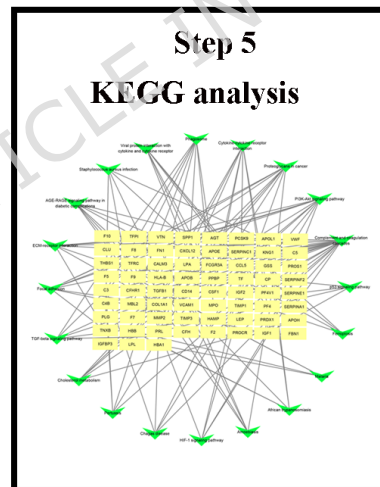
**A Drug targets**    **Disease targets**    **B 82targets**    **Proteomic targets**

**C Protein Class**

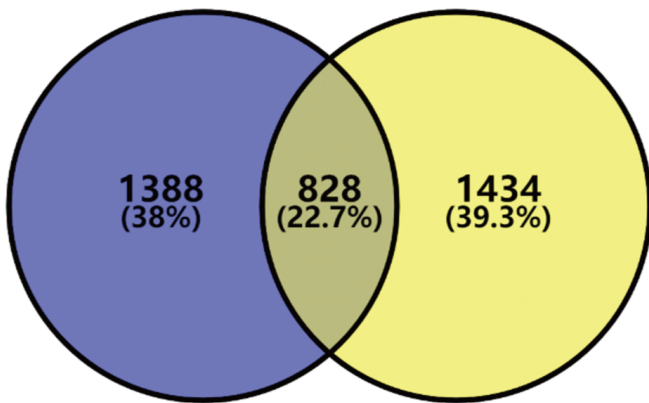
Protein Class	Percentage
Enzyme	34.1%
Transmembrane protein	23.1%
Cellular protein	14.4%
Extracellular protein	11.1%
Structural protein	10.1%
Signaling protein	8.1%
Transport protein	7.1%
Other	6.1%



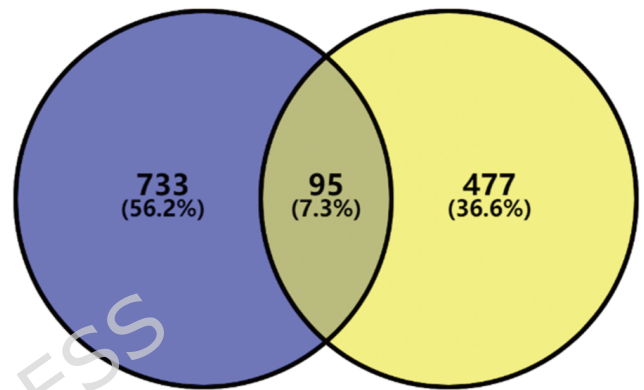
### Step 6 Molecular docking and MD simulations validation



**A Drug targets Disease targets**

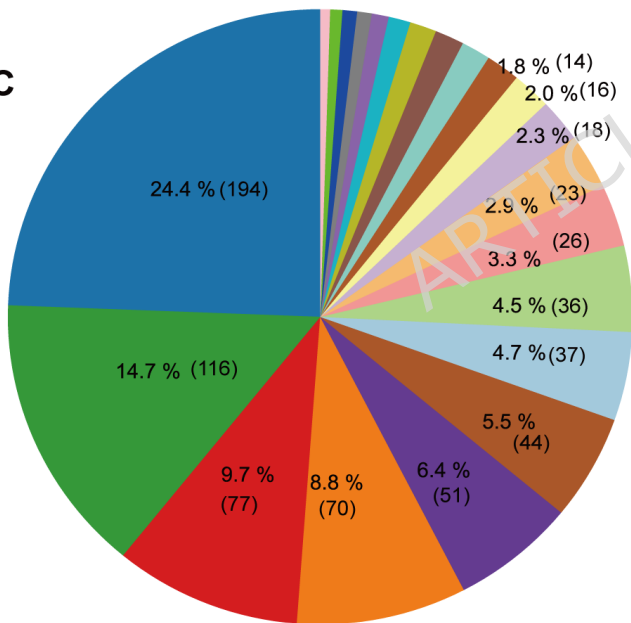


**B 828targets Proteomic targets**

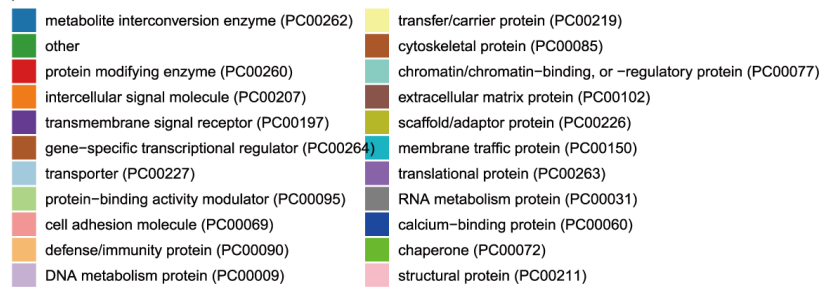


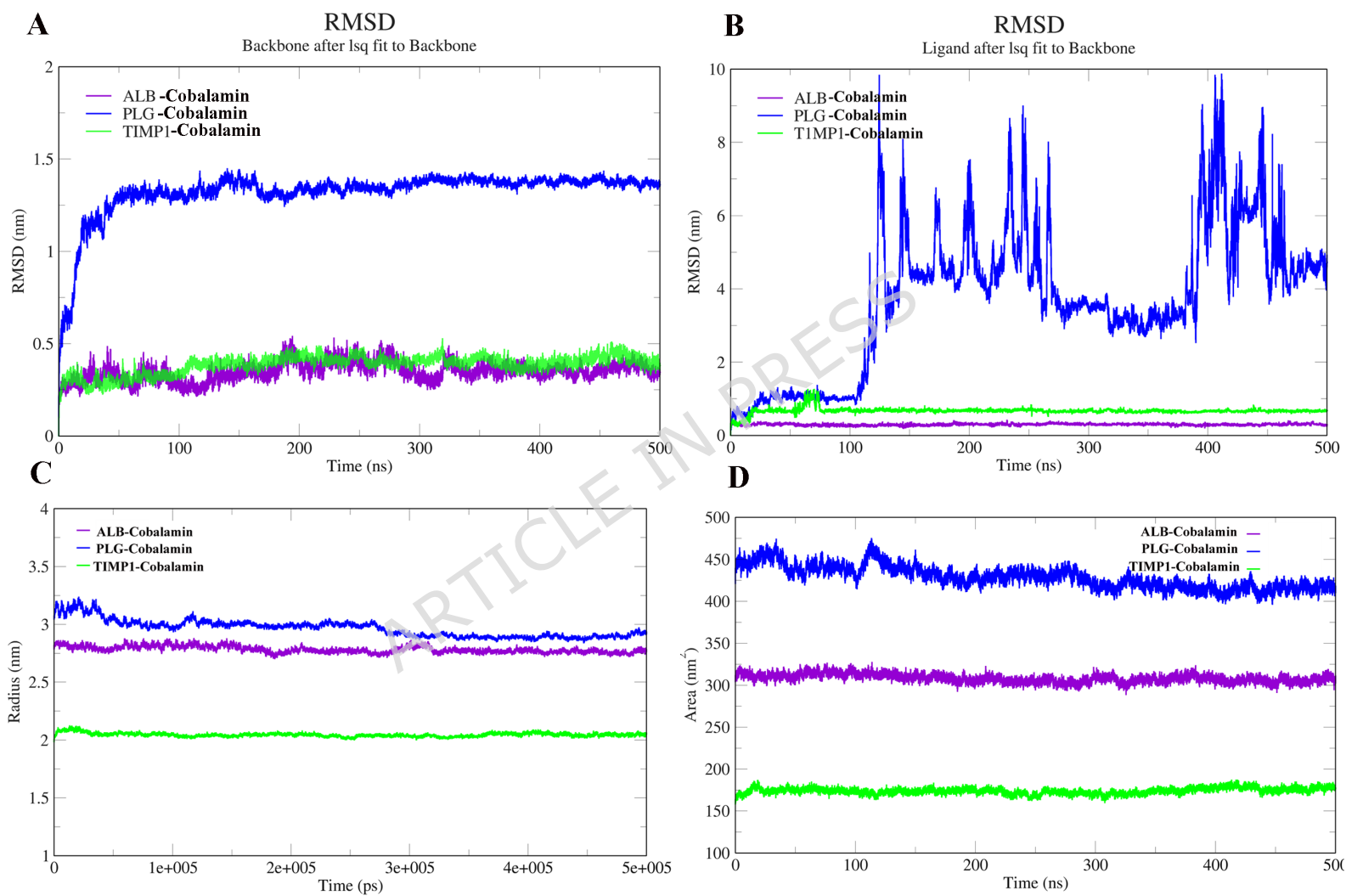
Protein Class

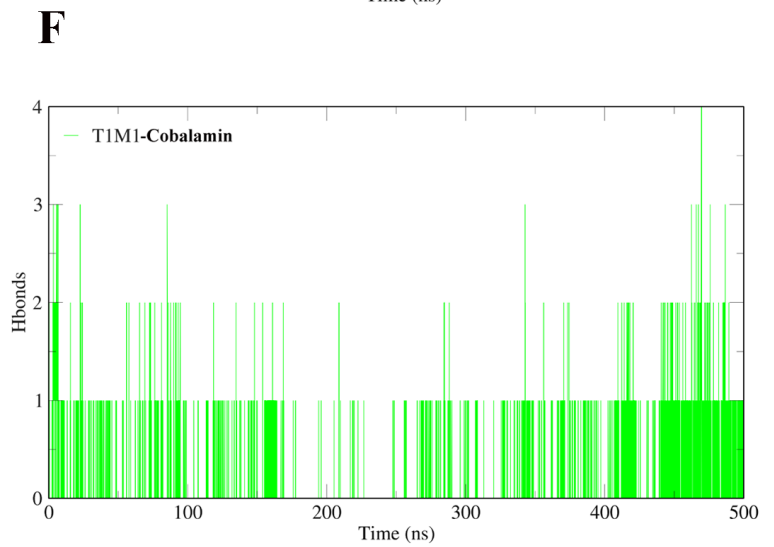
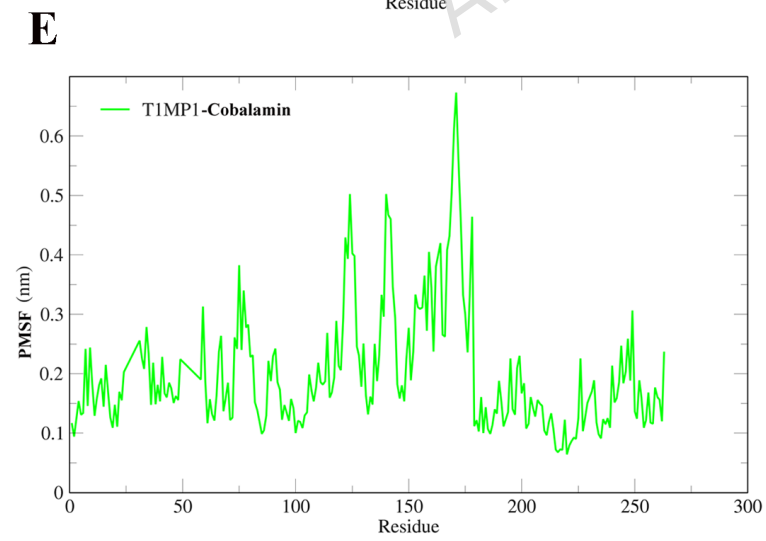
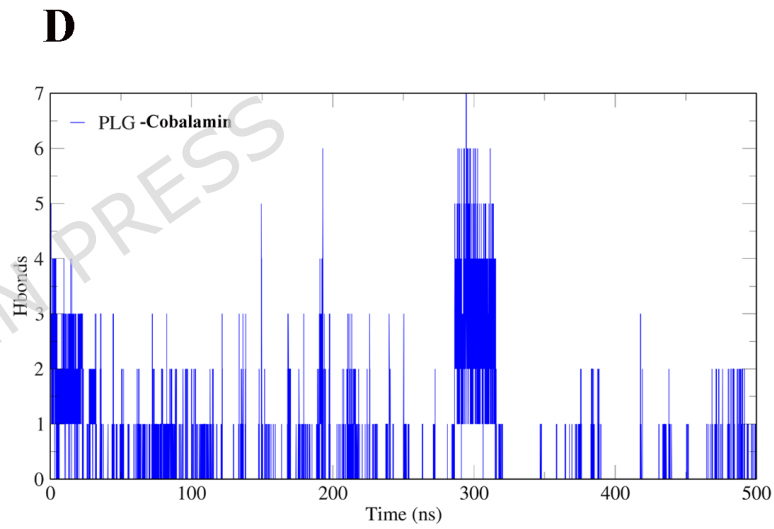
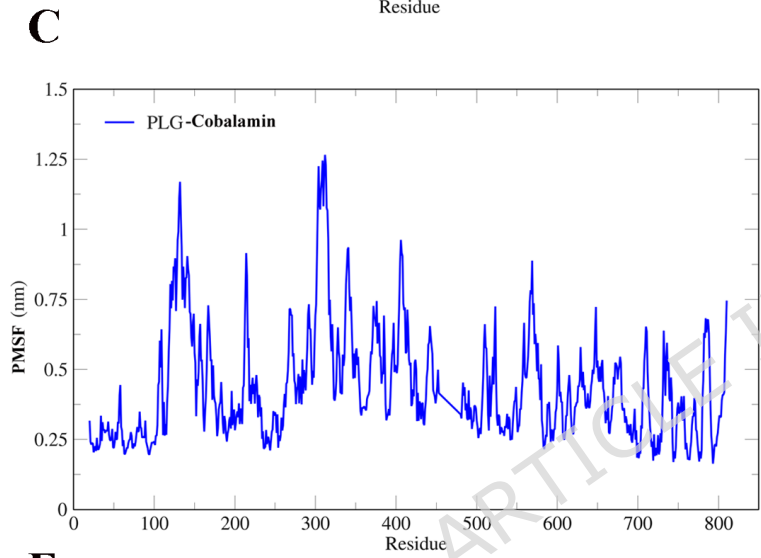
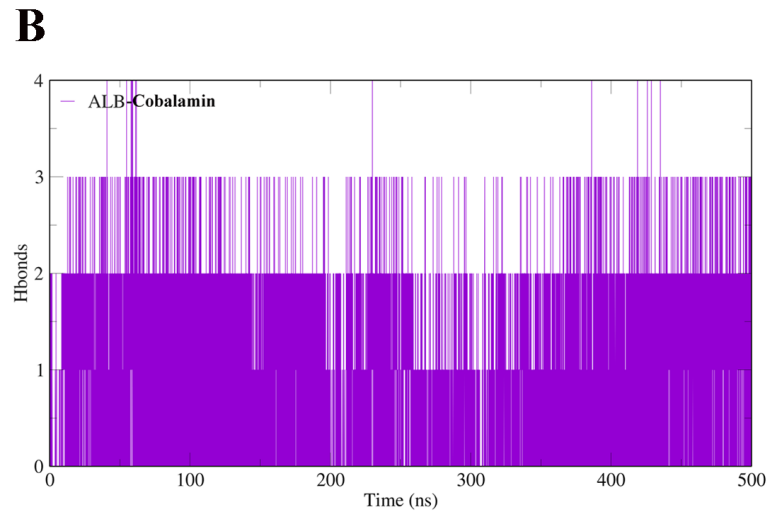
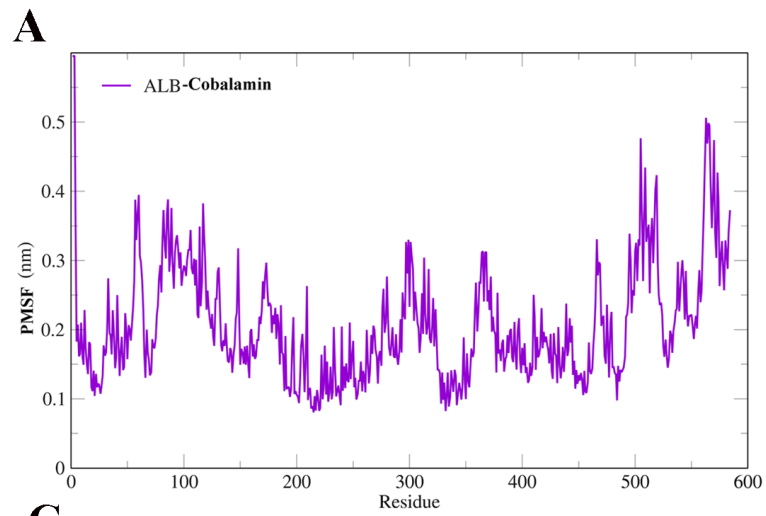
**C**

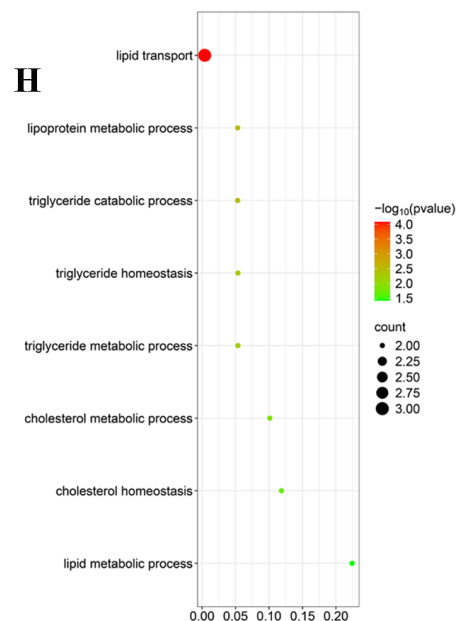
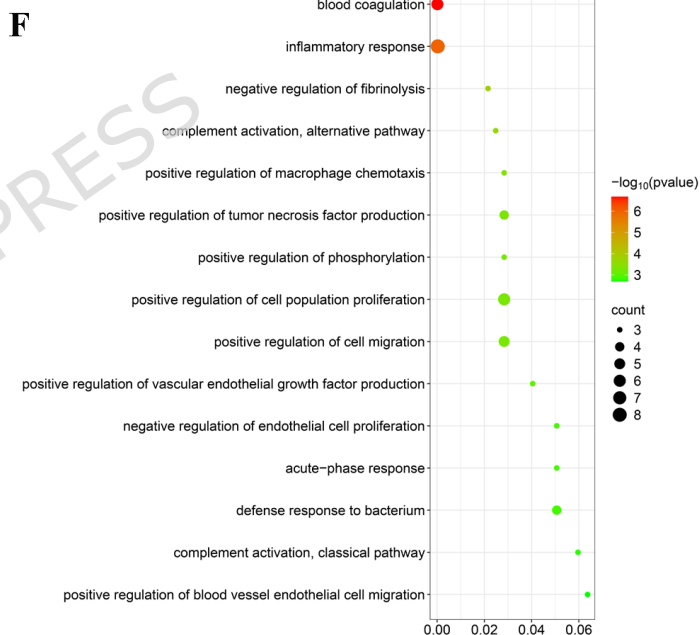
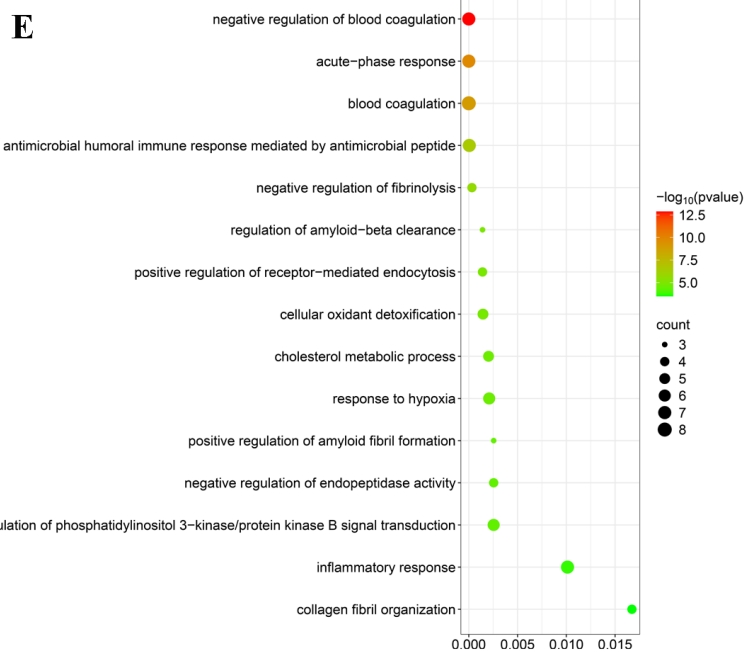
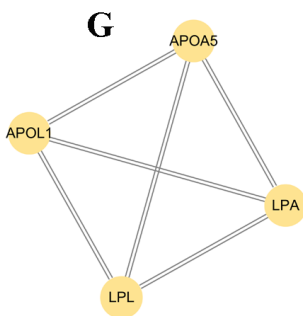
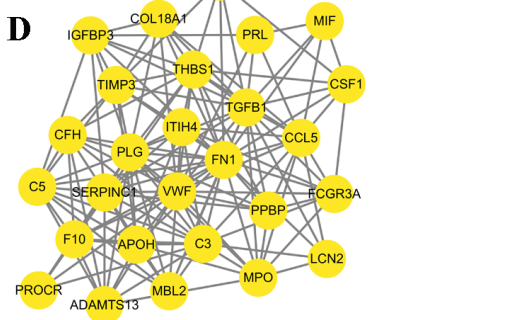
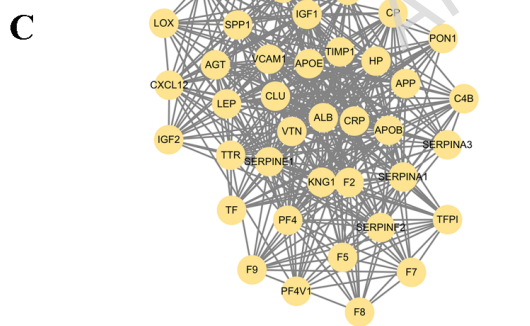
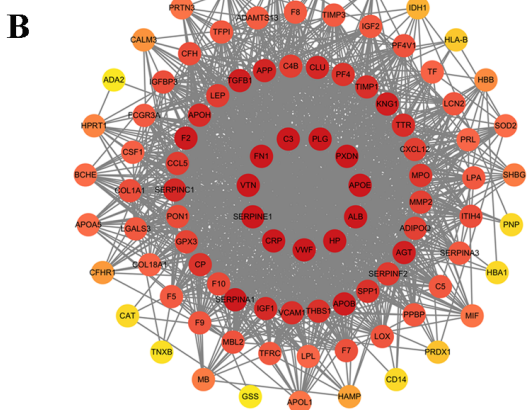
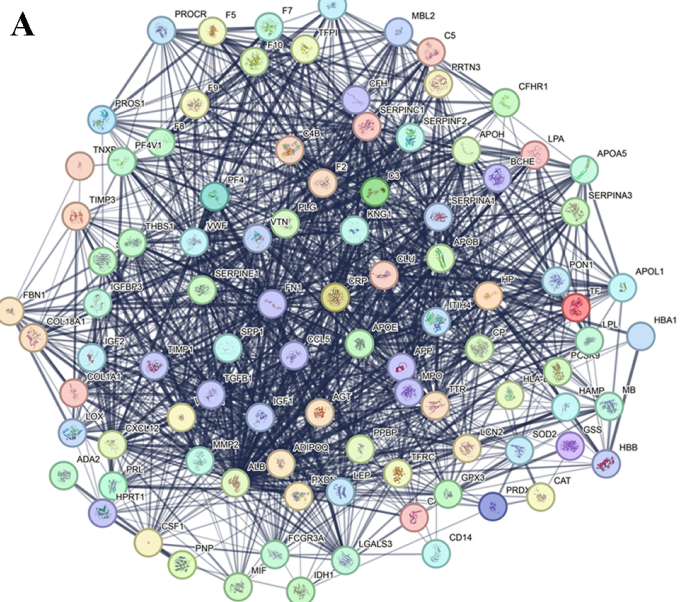


proteinclass

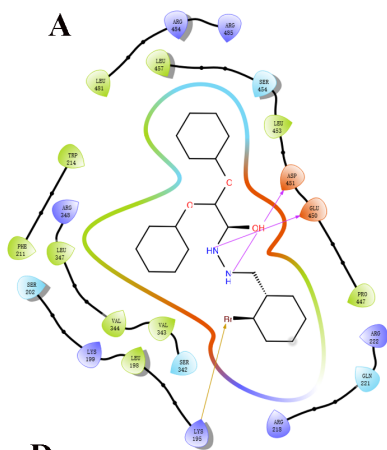
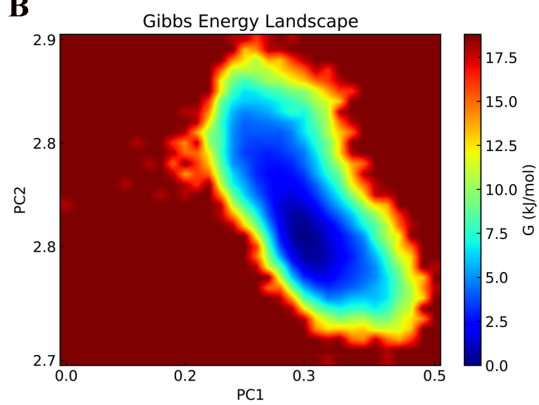
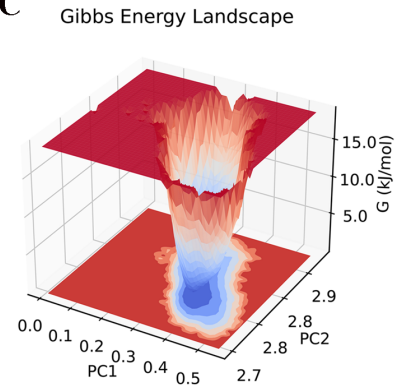
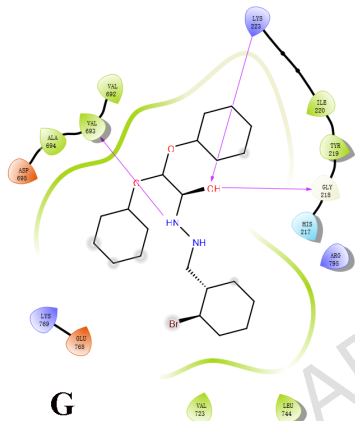
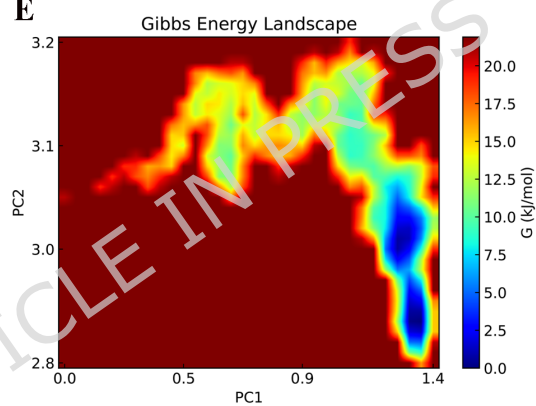
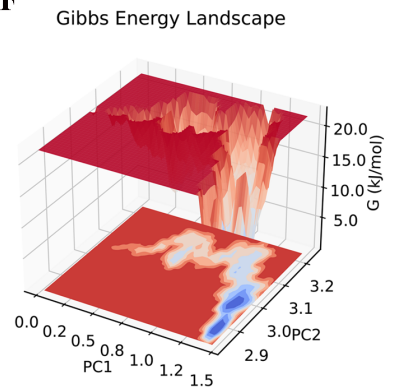
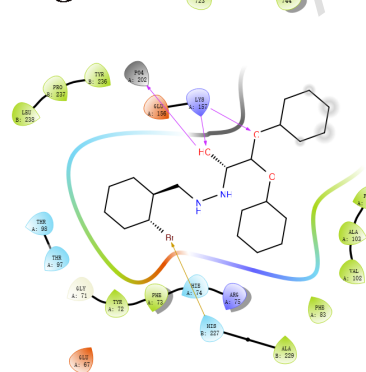
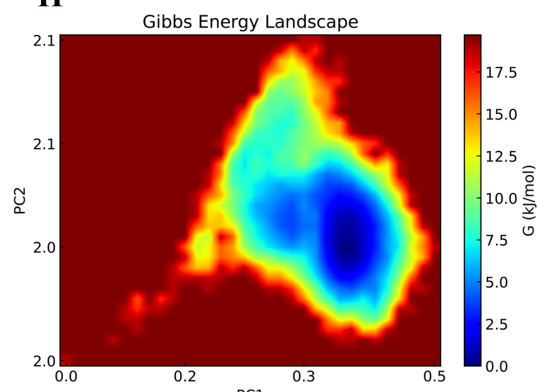
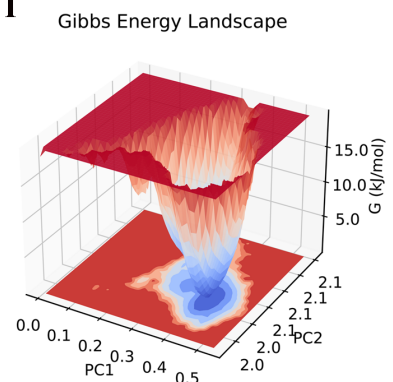






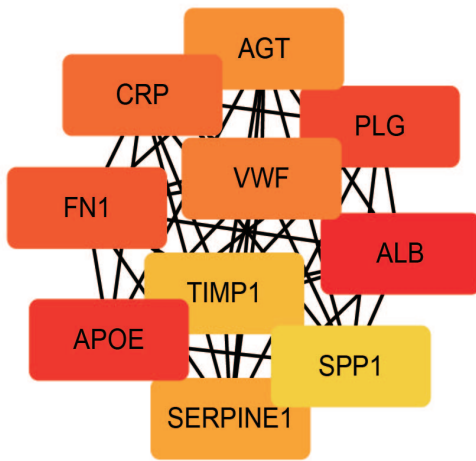


ALB

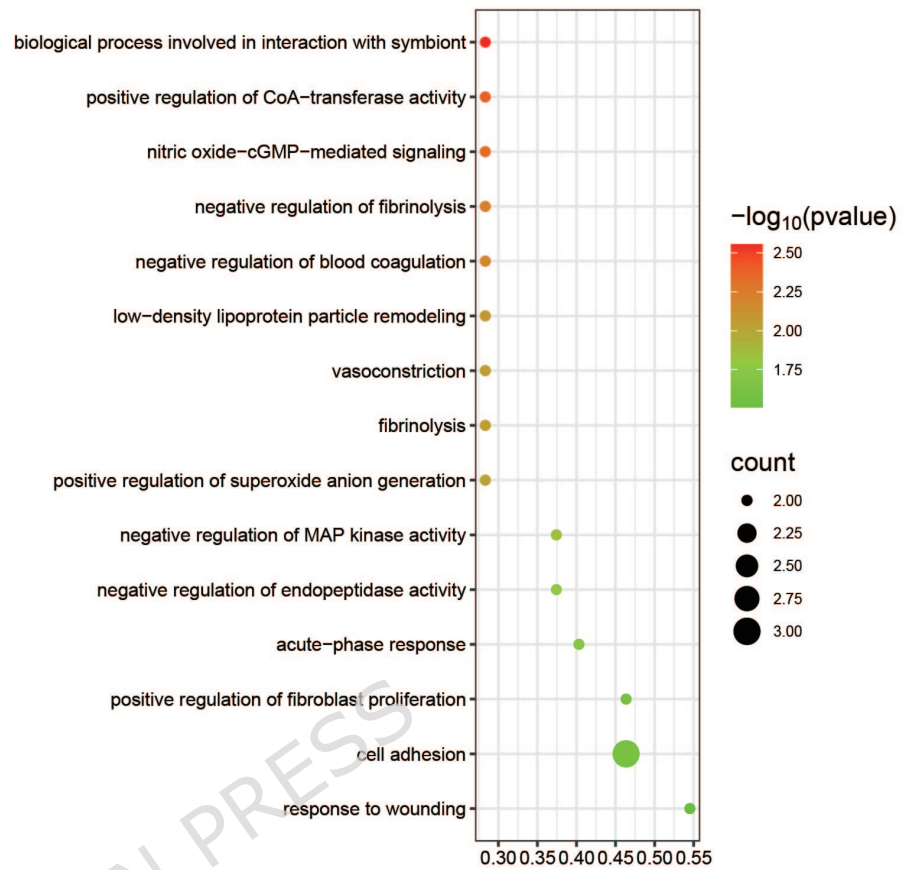
**B****C****D****E****F****G****H****I**

TIMP1

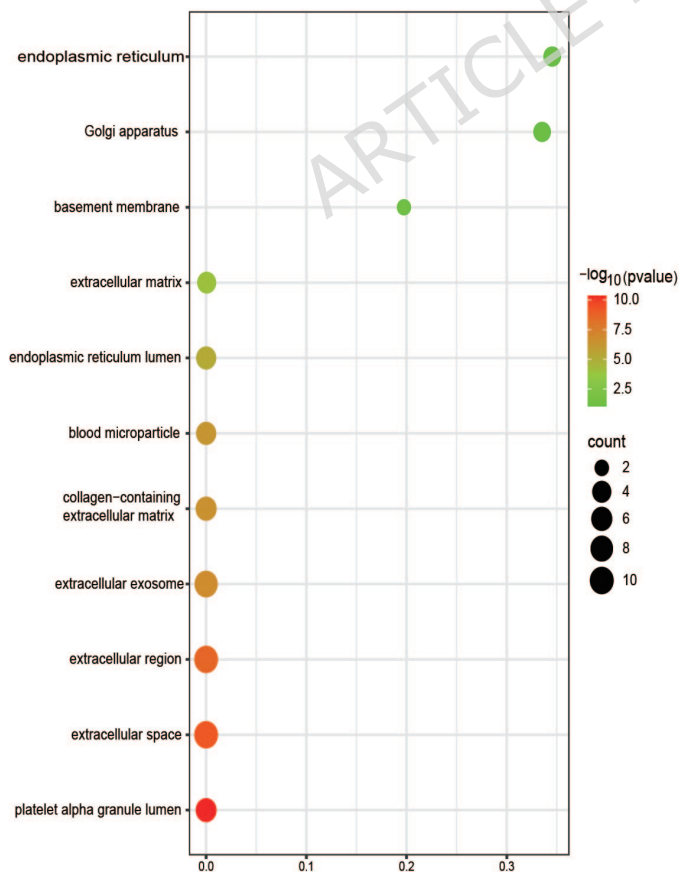
A



B



C



D

